Spring 2023

Load Rating Evaluation of Deteriorated Prestressed Channel Girders

Alexander Zane Henderson

LOAD RATING EVALUATION OF DETERIORATED PRESTRESSED CHANNEL GIRDERS

by

Alexander Zane Henderson

Bachelor of Science
University of South Carolina, 2022

Submitted in Partial Fulfillment of the Requirements

For the Degree of Master of Science in

Civil Engineering

College of Engineering and Computing

University of South Carolina

2023

Accepted by:

Paul Ziehl, Director of Thesis

Thomas Cousins, Reader

Fabio Matta, Reader

Cheryl L. Addy, Vice Provost and Interim Dean of the Graduate School

DEDICATION

To Jay and Jeanette, whose contributions and commitment to my academic journey have made my dreams reality. To Kyle, someone who inspires me more than anyone to dig deep when faced with obstacles. To Hannah, who I could not have achieved this accomplishment without.

ACKNOWLEDGEMENTS

This thesis is comprised of indirect and direct contributions made by numerous colleagues, mentors, friends, and professionals. First, I want to thank my mentor and supervisor Dr. Paul Ziehl, at the University of South Carolina. Dr. Ziehl is a highly-regarded and very respected member of the engineering community, and it has truly been an honor to work for him over the last two and half years. He has taught me many invaluable lessons, and showed me a level of professionalism I hope to achieve one day.

Second, I want to thank my research team: Dr. Li Ai, Elhussein Elbatanouny, and Laxman K C for all of the assistance they have provided in the laboratory. Their efforts are greatly appreciated.

I would also like to thank my committee members, Dr. Fabio Matta and Dr. Thomas Cousins, for their wise guidance and support throughout my time preparing this body of work and as a student while attending the University of South Carolina.

I would like to thank the South Carolina Department of Transportation, whom this research would not have been possible without.

I would like to thank the University of South Carolina for providing me the grounds for which to earn my education.

Lastly, I want to thank my family and friends for always believing in me while I pursued my education.

ABSTRACT

The South Carolina Department of Transportation (SCDOT) is conducting a multi-year effort to load rate its inventory of over 9,400 bridges. This includes many bridges that are load posted due to potential structural considerations (e.g., outdated design loads, members whose capacity is difficult to assess, structural degradation). The number of load-posted bridges in South Carolina is expected to increase significantly due to recent efforts from SCDOT to assess the current state of bridge infrastructure. It is expected that the increased scrutiny may result in more load postings, which in turn may lead to restrictions on truck routes, potential bridge closures, bridge repairs, and in some cases bridge replacement.

Initial findings have identified prestressed concrete skinny leg channels as one superstructure type that has difficulty meeting sufficient load ratings related to flexure. This thesis addresses skinny leg channel girders in their current state and their structural response up to failure to improve load ratings. The primary goal of this thesis is to contribute to the reduction of load restricted bridges in the state of South Carolina. Bridge load postings can be reduced by evaluating structural behavior of channel girders and tailoring load rating strategies to better represent behavior observed in the laboratory. Channels tested in the laboratory proved to be stronger than the nominal capacity, and this is attributed to higher than specified prestressing strand tensile strength and concrete compressive strength. However, some channels resulted in capacities below the nominal capacity, which is attributed to the structural deterioration. Two load rating

strategies were investigated and compared: Load and Resistance Factor Rating (LRFR) and Load Factor Rating (LFR). The LFR method proved to be the better method due to its superior performance for strength limit state and service limit state load rating.

TABLE OF CONTENTS

LIST OF TABLES

LIST OF FIGURES

LIST OF SYMBOLS

f'_c : Compressive strength of concrete.

f_u : Ultimate tensile stress

f_y : Yield stress

γ_{DC} : LRFD load factor for structural components and attachments

γ_{DW} : LRFD load factor for wearing surfaces and utilities

γ_P : LRFD load factor for permanent loads other than dead loads = 1.0

γ_{LL} : Evaluation live load factor

$\varphi_c =$ Condition factor

$\varphi_s =$ System factor

$\varphi =$ LRFD resistance factor

CHAPTER 1

INTRODUCTION

1.1 Problem

As of 2021, the percentage of bridges in South Carolina rated as structurally deficient is almost 11% and the national average is 7.5%. South Carolina contains 9,410 bridges in its inventory, with an average age of nearly 39 years old and fast approaching the typical 50-year service life. More of South Carolina's bridges are in fair condition (47%) than in good condition (45%), in accordance with Federal Highway Administration (FHWA) standards. 8% are inspected as in poor condition and 6.8% of bridges are load posted (South Carolina 2021). Figure 1.1 demonstrates the general trend of inspection ratings from 2012 – 2018 (SCDOT 2019). Figure 1.2 portrays the distribution of load posted bridges across the state (SCDOT 2019).

The transportation infrastructure in South Carolina includes many bridges that are load posted due to potential structural considerations (e.g., outdated design loads, members whose capacity is difficult to assess, structural degradation). The number of load-posted bridges in South Carolina is expected to increase significantly due to the recent rise in efforts from SCDOT to assess the current state of bridge infrastructure. As a result, the effort will have a negative economic impact due to limited truck routes, bridge closures, bridge repair, and bridge replacement. To mitigate increasing costs, methods to reduce load postings and bridge closure/replacement must be investigate.

The South Carolina Department of Transportation is conducting a multi-year effort to load rate its inventory of over 9,400 bridges. Initial findings from the effort have identified prestressed concrete skinny leg channels (referred to as "channels" hereafter) as one of the problematic superstructure types. Many channel bridges were not designed for the rating vehicles of today, and will require intervention in the form of posting, strengthening, or replacement. This thesis specifically addresses channel bridges in their current state and their structural response to failure in order to improve load ratings.

1.2 Specimen

In this thesis, precast prestressed concrete channel bridge girders, roughly 45 – 60 years of age, were investigated. This superstructure class was selected due to its quantity of sub-adequate load ratings as well as its relatively large portion of the superstructure population in the state of South Carolina.

1.3 Load Rating

Originally, load rating was used to convince the public that the bridges they were using were safe. Today, load rating still serves as a method to assess the permissible truck loads a bridge can safely carry (Alampalli et. al. 2021). Specifically, load rating is a way to quantify the live load capacity of structural components in a bridge system via a ratio of live load capacity and the live load demand. If the ratio is greater than 1, the bridge is suitable to carry the truck it was rated for. The lowest rated structural component of the bridge governs the load rating to represent a worst-case scenario (Sanayei 2016). Load rating is regulated by the American Association of State Highway and Transportation Officials Manual for Bridge Evaluation (AASHTO MBE). South Carolina Department of Transportation (SCDOT) utilizes the AASHTO MBE for load

rating requirements, with some adaptations to better suite South Carolina bridge infrastructure **(**SCDOT 2019**)**. Load rating is comprised of three different methods: allowable stress rating (ASR), load factor rating (LFR), and load and resistance factor rating (LRFR). The FHWA declares that all bridges designed after October 1, 2007 be rated using the LRFR method to promote nationwide standardization of the load rating practice (Sanayei 2015). Because the bridge girders examined in this thesis were designed some 50 years ago, the LFR method was used for load rating analysis to stay consistent with the time in which these girders were designed. However, the LRFR method was also investigated in order to compare the two rating methods and determine which one should be utilized to achieve a higher rating factor.

The conventional load rating methods can be modified by in-situ live load tests conducted with known truck weights to determine system response of superstructure members. Non-destructive testing (NDT) methodologies can be applied to record the elastic response of bridge superstructures, which then can be used to calibrate finite element models (FEM) or directly adjust rating factors by a modification factor (K). However, NDT usually requires temporary bridge closures, rerouting of traffic, more time for data processing, advanced equipment, and is more difficult than the conventional load rating techniques. NDT and FEM methods cannot be used on every bridge needing to be rated in the state. Thus, alternative adjustments to conventional load ratings must be developed to provide a more cost-effective approach. This can be achieved by acquiring a deeper understanding of the relationship between deterioration and capacity through laboratory testing and modifying load rating approaches to include this relationship more adequately.

1.4 Objectives

The investigations discussed in this thesis are a portion of a multi-year research effort explored by Clemson University (CU) and the University of South Carolina (USC) funded by SCDOT. The primary goal of this thesis is to contribute to the reduction of load restricted bridges in the state of South Carolina.

Specific goals of the thesis include:

- Identify and classify typical deterioration in channel girders before testing.
- Determine flexural behavior and capacity through experimental testing.
- Determine concrete compressive strength and prestressing strand tensile strength and compare to their respective specified strengths.
- Identify relationships between existing deterioration and measured girder capacity.
- Compare LRFR rating method to LFR rating method.
- Compare nominal capacity load rating to measured capacity load rating.

1.5 Layout of Thesis

This thesis is composed of five chapters and an appendix. Chapter 2 is a literature review of different prestressed concrete girder testing and load ratings. In Chapter 3, the methodologies of the experiment are presented. Results and discussion of the tests are presented in Chapter 4, followed by conclusions and future work in Chapter 5.

1.6 Figures

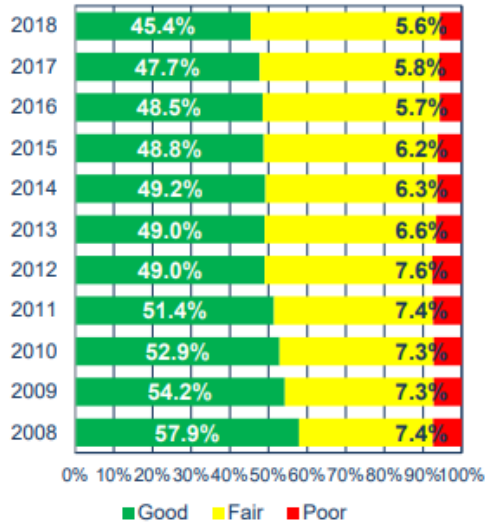

Figure 1.1 NHS bridge condition based on federal metrics percent by count (SCDOT 2019).

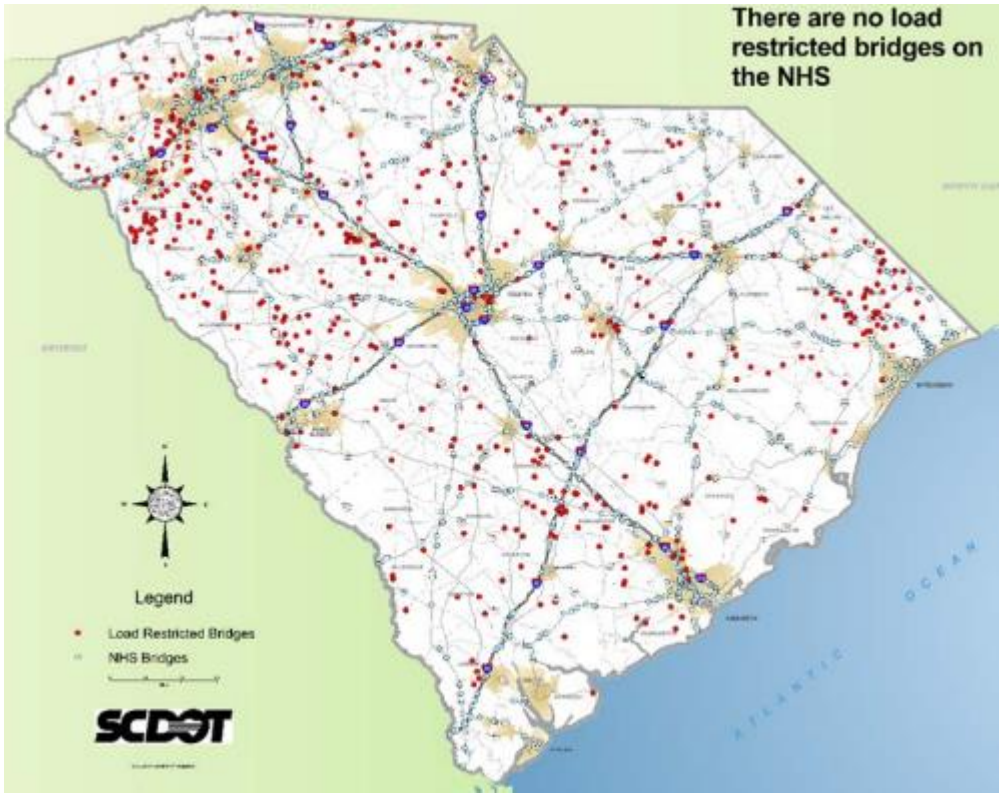

Figure 1.2 Load restricted bridges as of February 12, 2019 (SCDOT 2019).

1.7 References

Alampalli, S., Frangopol, D. M., Grimson, J., Halling, M. W., Kosnik, D. E., Lantsoght, E. O. L., Yang, D., & Zhou, Y. E. (2021). Bridge Load Testing: State-of-The-Practice. Journal of Bridge Engineering, 26(3), [03120002]. https://doi.org/10.1061/(ASCE)BE.1943-5592.0001678

Sanayei, Masoud & Ford, Alexandra & Brenner, Brian & Imbaro, Rosalind. (2015). Load Rating of a Fully Instrumented Bridge: Comparison of LRFR Approaches. Journal of Performance of Constructed Facilities. 30. 04015019. 10.1061/(ASCE)CF.1943-5509.0000752.

South Carolina: ASCE's 2021 infrastructure report card. ASCE's 2021 Infrastructure Report Card |. (2021, September 13). Retrieved February 7, 202.3, from https://infrastructurereportcard.org/state-item/south-carolina/

South Carolina Department of Transportation. (2019). *Load Rating Guidance Document*. https://www.scdot.org/business/pdf/bridgemaintenance/loadrating/SCDOT-BridgeLoad-RatingGuidance-Doc-NoHigh.pdf

South Carolina Department of Transportation. (2019). *Transportation Asset Management Plan*. https://www.scdot.org/performance/pdf/reports/TAMP.pdf

CHAPTER 2
LITERATURE REVIEW

2.1 Channel Girders and Existing Deterioration

Structural evaluation of SCDOT prestressed channel bridges

Gunter (2016) analyzed structural characteristics of prestressed channel bridges in South Carolina through live load tests in the field, laboratory destructive testing, and analysis. Channel girders act as components of a superstructure system typically composed of 11 girders that are 30 feet in length. The live load field tests were conducted on the Five Forks Bridge in Liberty, SC which is comprised of 33 girders that form three simple spans each 30 ft. long. Laboratory testing was conducted on a girder like those of Five Forks Bridge. Material properties of the bridge were unknown, leading to assumption of properties like concrete compressive strength and prestressing strand yield strength determined by SCDOT drawings of similar superstructures.

Deterioration to Five Forks Bridge was recorded via visual inspection. The results of this inspection show the West span possessed a deteriorated exterior girder. The West span girder displayed evidence of strand corrosion, which led to multiple inches of concrete spalling and exposed strand. The remaining East and Middle spans contained no deteriorated girders.

Live load tests were conducted on the Five Forks Bridge using different truck weights ranging from “light” loads to the legal limit for the bridge. Behavior of the deteriorated girder was compared to the behavior of other non-deteriorated girders under

various truck loads, where strain and deflection were recorded using linear variable differential transformers (LVDTs) and Bridge Diagnostic Inc. (BDI) strain gauges. Due to difficulty loading the exterior girder, it was inconclusive whether or not there were any effects of deterioration.

An identical surplus girder, in good condition, obtained from SCDOT was tested to failure in the laboratory to compare to the load-deflection behavior of the Five Forks Bridge girders. Specifically, a direct comparison of strain recorded in the live load field test and surplus girder laboratory was used to determine the impact factor (IM) used in the LRFR load rating equation. This surplus girder was tested in a 4-point bend configuration and simply supported. The instrumentation for the surplus girder test was similar to that of the live load field tests.

Results of the testing show that deflection data in the live load tests had unexplained errors and therefore could not be used in the analysis. Strain served to calculate impact factor (IM), moment distribution factor (DFM), and load rating modification factor (K) to produce a more accurate load rating. The surplus girder testing displayed a moment-deflection plot which corresponds to a self-weight moment of 40 kip-ft., cracking moment of 150 kip-ft., and nominal moment of 324 kip-ft. Differences in strain from the live load testing and surplus girder testing were used to determine IM. Experimental IM was less than one for girders directly under load, indicating a non-conservative estimate and therefor was not used in the load rating equations. Bridge girders in the live load field tests were stiffer than the surplus girder. AASHTO LRFD strain and ultimate strength calculations and less than the experimental capacity measured in the laboratory test.

Conclusions from Gunter (2016) are as follows:

- Bridge geometry prevented full loading of the deteriorated exterior girder resulting in an unclear understanding of the effects due to deterioration.
- Individual girders had 3% more strength than AASHTO LRFD equation suggested.
- Experimental IM was less than 1 and therefor unusable.
- A legal modified load rating factor greater than one was achieved and therefor the Five Forks Bridge does not need to be posted.

The girder material properties, location, service life, nature of deterioration, and experimentation in Gunter (2016) are very similar to the findings presented in Chapter 3 and beyond in this report.

Experimental evaluation of precast channel bridges

Klaiber et al. (2003) investigated precast channel bridges girders from secondary road Iowa bridges built some 40-50 years ago. Many of these bridges (600) show signs of deterioration. Typical deterioration consists of reinforcement corrosion resulting in spalling or missing concrete cover, cracking, and rust stains on the bottom of the soffit. This type of deterioration leads to loss of cross-sectional area in the reinforcement and ineffective reinforcement-concrete bond. Four channel bridges were instrumented in the field with deflection transducers and strain gauges to track midspan vertical deflections and strains during truck loading. Twelve laboratory tested girders were loaded to failure in a four-point bend test set-up and were instrumented similar to the four field tests. The overall goal of Klaiber et al. (2003) was to assess the structural sufficiency of the girders' deteriorated state through field and laboratory testing.

Four deteriorated precast concrete channel bridges were tested in the field to determine the effectiveness of shear key load distribution in the bridge spans. Midspan deflection and strain were recorded to determine load distribution, which is the main function of the shear keys. These instruments were also utilized to determine if the girders were loaded above or below their allowable stress limits. Due to weather and traffic conditions, accurate strain measurement was only captured from Bridge 2. Bridge 2 experienced the largest compressive strain of 110 με, corresponding to a maximum stress of 7.67 kPa which is below the specified maximum allowable stress limit (13.8 kPa). Bridge distribution factors were calculated by comparing individual girder deflections to the remaining girder deflections. The controlling distribution factor was linked to the girder directly under the wheel load. Distribution factors varied amongst the four bridges due to the different states of the shear keys. Typical shear key construction for these bridges consists of two different types: Type 1; continuous grouted shear key with transverse bolts, and Type 2; concrete filled galvanized pipe with transverse bolts. Bridge 3 (Type 1) and Bridge 1 (Type 2) both had the lowest distribution factors of the four bridges. The lower the distribution factor the better the distribution of live load on the bridge. As distribution factor decreases, reductions in applied load increase and therefore increase load rating. The distribution factors calculated from deflection data are 0.42 and 0.49 for Bridge 3 and Bridge 1 respectively. Both are less than the AASHTO calculated design distribution factors of 0.58 and 0.57 respectively. The results verify the effectiveness of shear keys in good condition. Bridge 2 is a good example of shear keys in poor condition, with a distribution factor of 0.68, which is greater than the design

distribution factor of 0.56. The controlling girder is supporting 21% more load than designed for.

Twelve deteriorated channel girders from three different decommissioned bridges were tested to failure to determine ultimate flexural capacity. Girders varied from 7-11 m. The deteriorated state varied for each girder. Typical deterioration consisted of corroded reinforcement which led to spalling. Some girders exhibited extreme signs of deterioration, with the majority of the primary reinforcement exposed and severely corroded. This can be seen in Figure 2.1. Instrumentation was similar to the four bridges tested in the field. Each girder was tested in a 4-point bending arrangement with 1.8 m separating the applied load points. After testing, concrete cores and prestressed strands were removed to determine existing compressive strength and yield strength. Results of the testing show that the channel girders performed well despite their deteriorated state. Generally, experimental capacity exceeded theoretical capacity. This can be attributed to three main factors. First, the primary reinforcement possessed large hooks at each end of the girders which made concrete-reinforcement bond issues due to spalling negligible. Second, the girders possessed material properties much higher than specified, due to factors of safety implemented in the design process. Third, strain hardening effects allow for steel stress limits to be greater than the idealized stress plateau at yielding utilized in typical reinforced concrete theory. The failure mode was concrete crushing at the top of the girder. A summary of the flexural tests results is presented in Table 2.1 which lists the county the girders were recovered from and the comparison of experimental to nominal capacity. The Cedar girders presented in the table demonstrated the highest capacity while having the shortest span length. This phenomenon occurred due to higher

than specified concrete compressive strength and significant strain hardening effects. The Butler-3 girder experienced the lowest capacity of the tested population. Butler-3 was the most significantly deteriorated girder, leading to decreased capacity and the only test that resulted in experimental capacity below the theoretical capacity. Heavy spalling and corrosion of primary reinforcement was evident. Roughly 50% of the girder deck surface was delaminated and spalled. Reductions in cross-sectional area of the girder and its reinforcement directly affect the moment arm of the section and available tensile strength of the reinforcement.

Conclusions of the various tests conducted in Klaiber et al. (2003) are described as the following:

- The most common form of deterioration was corrosion of the primary reinforcement and spalling of the concrete cover.
- Both the laboratory and field testing demonstrate that the deterioration had minimal effects on the performance of these bridge girders. Only very severe deterioration to the girder led to a significant impact on capacity, as evident in the Butler-3 test.
- The shear connections between girders affected the performance of the superstructure system. Poor shear connections led to distribution factors less than required by AASHTO, resulting in increased live load effect to individual girders and decreased load rating.

An autopsical examination of 40-year-old pre-tensioned concrete bridge girders

Mills (2010) investigated the performance of six prestressed concrete channel girders collected from the Canadian National Railway overpass on the Trans-Canada

Highway No. 1 east of Portage La Prairie, constructed in 1965. The girders exhibited various levels of deterioration across the decommissioned bridge, mainly due to freeze-thaw effects. The objective of the report was to experimentally determine the residual capacity of the girders given their deterioration state.

Girder dimensional properties consisted of 19,810 mm in length, 864 mm in depth and 1,219 mm in width. Flange depth and bottom web width were 152 mm. Design compressive strength was 37.9 MPa. Twenty-13 mm diameter prestressed strands were stacked in two columns of ten with a vertical spacing of 50 mm and 50 mm of cover at the soffit of the web. An additional 14 prestressed strands (also 13 mm) configured in a single row of one and three rows of two were draped, with 50 mm of cover above and on the exteriors of the webs as well. All strands were 7-wire strands with design tensile strength of 1,724 MPa. Compression reinforcement consisted of five 13mm bars, with three located at the top of the flange and two located at the bottom of the flange. All compression reinforcement contained 50 mm of cover above or below. 13 mm U-shaped stirrups served as the shear reinforcement. Girders also contained diaphragms at the third points of the span.

All six channel girders were visually inspected to determine deterioration prior to testing. All girder deterioration observed was similar in nature but the severity of damage among all specimens varied. Girder condition was categorized into three families: good, fair, or poor. Good rating signified no horizontal cracking or concrete cover loss at or near the soffit of the legs. Fair rating indicated minor horizontal cracking and no significant concrete cover loss. Finally, poor rating showed significant concrete

cover loss which aided in development of notable strand corrosion. Table 2.2 summarizes the condition and characteristics of deterioration for each of the six girders.

Experimental set-up consisted of a 3-point bend configuration, simply supported at both ends with the center lines of each bearing at 457 mm from each end of the girder. Load was applied at the girder longitudinal and transverse center lines with a hydraulic actuator. LVDTs were placed at L/6 to measure vertical displacement. Three strain gauges were utilized at intervals of 3150 mm with two on the bottom of the web soffits and one on top of the girder center on their respective width dimensions. A load cell continuously measured applied load during the tests. Monotonic load was applied in steps of 50 kN to 400 kN, then steps of 25 kN were applied until failure. Three girders were tested for flexural capacity and the other three girders were tested for shear capacity. The girders tested for shear capacity are not discussed in the review of this article due to their lack of relevancy to the tests performed in the following chapters.

Results of the flexural tests show that girders 1-3 failed at an experimental moment of 3,577 kNm, 3,462 kNm, and 3,224 kNm, respectively. Nominal moment capacity was calculated as 2,771 kNm for girder 1 and 2, and 2,565 kNm for girder 3 based on 50 mm of missing cover and 2 ineffective strands. Girders 1-3 had a 29%, 25%, and 26% higher capacity when compared to the theoretical capacity. Girder 3 was the only girder of the flexural tests that contained significant deterioration. Despite roughly 50 mm of concrete cover loss and 2 strands considered ineffective, the girder performed well above the theoretical capacity. This makes sense considering actual material properties of the girders were higher than the design properties due to incorporated factors of safety in design. Cylindrical cores were taken from all 6 girders with adjusted

average core compressive strength being 51.5 MPa, roughly 36% higher than the specified design value of 37.9 MPa. Failure mode consisted of an explosion of the compression zone resulting in a non-ductile failure and complete collapse of the girders.

Load rating analysis was conducted using the Canadian Highway Bridge Design Code (CHBDC) and AASHTO LRFR methods. Due to relevancy, only the results of the AASHTO LRFR method will be summarized in this paragraph. Load rating assumptions utilized HS-20 and HSS-30 design loads, dead load factors of 1.25 and 1.50 for self-weight and wearing surface respectively, inventory and operating live load factors of 1.75 and 1.35 respectively, and an impact factor of 1.33. A value of 1.0 was used for flexural resistance factor and system factor. Condition factors of 1.00, 0.95, or 0.85 were used for girders based on their categorization of either good, fair, or poor condition displayed in Table 2.2. Experimentally tested girder load ratings utilized condition factors, even though the capacity of the girders should reflect their condition and therefore increase the conservativeness of the experimental load ratings. A comparison of nominal to experimental load rating is summarized in Table 2.3, which shows that experimental rating factor is significantly greater than the nominal rating factor. All three girders had an experimental load rating greater than one for the HS-20 truck. The HSS-30 truck load caused experimental load ratings less than one for girders two and three.

Conclusions of the various tests conducted in Mills (2010) are described as the following:

- All girders performed better than their nominal calculations despite their deterioration.

- Superior girder strength compared to nominal strength was due to conservatism within the Canadian and American design codes.
- Under AASHTO LRFR guidelines, all of the girders received a nominal and experimental rating factor greater than one for HS-20, and not HSS-30. Girders 2 and 3 did not receive an experimental rating factor greater than 1 for HSS-30 design load.
- Experimental rating factor was significantly greater than nominal rating factor.

2.2 Bridge Load Rating

Capacity and load rating of in-service precast prestressed concrete bridge deck girders with transverse cracks

Gunasekaran et. al. (2023) investigated one prestressed precast concrete (PPC) box beam that had been in service for over 37 years to determine the effects of transverse cracks on flexural performance. The PPC girder was taken from a bridge in Schuyler County, Illinois constructed in 1984. The study specifically addressed the impacts of transverse cracks on the girder and the associated decreased capacity and load rating due to the numerous adverse effects transverse cracks can cause. The objectives of this study were to investigate the post-crack behavioral effects and quantify residual capacity, study the serviceability effects of crack width, and investigate the impact of transverse cracks on load rating.

The test specimen obtained was a 33 in. by 36 in. PPC box girder which served as the driving deck (no cast-in-place slab or asphalt wearing surface). This exterior girder was selected from the site due to its transverse crack which propagated from the bottom of the girder to the top surface. The girder plan and cross-section can be seen in Figure

2.2. Nominal moment capacity of the girder was calculated under AASHTO MBE guidelines and was determined to be 720.5 kip-ft., assuming 20% prestressed strand losses. Subtracting a 179.7 kip-ft. self-weight moment, the applied nominal capacity was determined as 540.8 kip-ft.

A finite element model (FEM) was used to determine theoretical load-deflection behavior which was compared to the experimental load-deflection results. The FEM also helped determine theoretical load rating results further discussed in later paragraphs. The FEM assumptions were derived based on the girder characteristics and properties.

Experimental full-scale set-up consisted of a four-point bending configuration simply supported by a roller and pin. Load applied by a hydraulic actuator was displacement controlled at a rate of 1 mm/min. The rate was doubled after the girder load-deflection response plateaued. The two points of load contact were two 50 mm by 25 mm by 37.5 mm plates with a clear spacing of 4.5 ft. to simulate tandem axles. The two plates matched the 10 degrees skew the girder was designed with. One linear variable differential transformer (LVDT) and two string potentiometers were employed at midspan to measure displacement. All existing cracks were identified, marked, and widths were measured prior to testing. A total of 21 strain gauges were attached to the girder to determine strain at various locations along the cracks, as well as strains in between cracks.

Results of the test can be seen in the load-displacement curve shown in Figure 2.3. The girder demonstrated linear behavior up until a load of 30 kips and 0.25 in. midspan displacement. Crack C6 then propagated beyond the soffit of the girder, and once the behavior became non-linear crack C6 began to open and multiple new cracks

formed. All the dips in the load-deflection curve in Figure 2.3 are attributed to the opening of a new crack or propagation of an existing crack. Load increased up to 59.2 kips and 3.7 in. of displacement was reached, where ultimate capacity was achieved and complete failure occurred. The failure mode consisted of concrete crushing followed by strand rupture. The noticeable difference between the experimental and FEM load-displacement response were thought to be due to existing cracks and concentration of stresses in the prestressed strands at these crack locations.

Load rating was conducted in accordance with the AASHTO LFD method. Capacity and serviceability rating factors were conducted for both the experimental (cracked) test results and theoretical (uncracked) as-built condition from the FEM. A summary of the rating factors is presented in Table 2.4. Equations (1)-(6), referred to in Table 2.4, were obtained from AASHTO MBE and are in accordance with the LFD method. An analytical model from Rao and Dilger (1992) was utilized to estimate the effect of crack width on strand stress increase and concrete compression stress increase. This analytical model was used to demonstrate how transverse cracks can affect load rating by causing stress build-up in prestressing strands and the concrete compression zone. As a result, all the experimental load factors were adjusted in accordance with the results of the analytical model. This is why the inventory prestressing steel tension rating factor for the tested girder was a negative value.

Conclusions from Gunasekaran et. al. (2023) are described as the following:

- Residual capacity and ductility of the tested girder are 46% and 56% less than the FEM results, respectively. The tested girder demonstrated early non-linear behavior compared to the FEM results.

- The tested girder load rating capacity was reduced by 34%, resulting in inventory and operating rating factors to be decreased by 22%.
- According to various analytical models from literature, transverse cracks may cause an increase of up to 29% in prestressing strand stress, which resulted in the inventory rating factor being less than zero.
- Serviceability load rating factors were highly sensitive to stress build-up in the prestressing strands, which is related to the width of the cracks.
- Despite a serviceability rating factor being below zero, the tested girder was able to carry over 50% of its nominal capacity while still within the elastic range. This demonstrates that the bridge owner may decide to load post bridges of this nature based on capacity rather than serviceability rating factor equations.

Load rating of a fully instrumented bridge: comparison of LRFR approaches

Sanayei et. al. (2015) investigated the Powder Mill Bridge through Vernon Avenue in Barre, Massachusetts. Powder Mill Bridge is a three-span continuous concrete slab on steel girder bridge. The test led to comparisons of different load rating approaches to determine improved rating factors. The bridge is located close to Barre-Martone regional landfill and recycling center which ensures heavy truck traffic frequently passing over the bridge. The bridge is comprised of six steel girders, with interior girders being W36 x 160 and the two exterior girders are W36 x 232. The purpose of this paper was to compare conventional load rating techniques to nondestructive testing (NDT) and finite element modeling (FEM) techniques to better represent bridge system behavior and improve load rating.

The AASHTO LRFR approach was utilized in load rating the Powder Mill Bridge using three different techniques: conventional load rating using a simplified line girder analysis, conventional load rating adjusted by NDT data, and 3D FEM analysis load rating. The main difference in these three approaches lies within the live load distribution factor. Live load distribution factor is a way of quantifying the share of live load received by each individual girder. Due to a prioritization of safety, the conventional load rating method results in a conservative live load distribution factor. The purpose of the non-conventional methods is to better determine load share among these girders to produce a less conservative load rating result.

The Powder Mill Bridge consists of six steel girders previously discussed, configured in 3 continuous spans requiring rating factors to be calculated for the positive and negative moment regions of the spans. Negative moment region controlled the rating, therefor the results presented are only representative of the negative moment region in question. Rating assumptions consist of superimposed dead loads due to railings, barriers, and sidewalks being distributed as 60% of the load to the exterior girders and 40% of the load to the interior girders per Massachusetts Department of Transportation. The wearing surface was distributed uniformly across all girders. Unit weight of concrete was assumed to be 150 lb./ft^3 which is typical. All adjustment factors for the LRFR rating equation are considered standard for inventory and operating loads and are in accordance with AASHTO.

Adjustments to the conventional load rating method were conducted through nondestructive testing, which was performed at the Powder Mill Bridge on September 25, 2011. No deterioration was observed, therefor the comparison of all three bridge load

ratings is a pure comparison of levels of conservativeness built into the load rating procedure. The National Cooperative Highway Research Program (NCHRP) provides assistance for NDT load rating and these guidelines were utilized in the procedure. A triaxle dump truck weighing 79.48 kip was driven across the bridge on six different load paths to sufficiently stress each girder. Due to the sidewalk over girder six, the girder was not sufficiently stressed to validate the NDT adjusted rating. Strain gauges were applied 1 m from the maximum positive bending moment. This strain data was used in the calculation of live load distribution and the rating adjustment factor (K). Live load distribution factors for each girder were compared to theoretical AASHTO distribution factors, and it was determined that the AASHTO distribution factors led to a more conservative result and were therefore used in the NDT adjusted procedure. A summary of the NDT rating factors can be found in Table 2.5.

The last load rating method utilized in the study was the finite element model (FEM) approach. The original model utilizes all the design properties associated with the bridge materials and matches all of the dimensions associated with the actual bridge. However, the model was calibrated using results from concrete cylinder strength tests, live load tests, additional parapet stiffness, and reduced concrete stiffness in the negative moment region due to cracking. Strain data collected in the NDT evaluation was used to verify the FEM. In order to inflict the worst-case scenario for each girder, three loading lanes were considered in the FEM and the sidewalk was removed from the driving surface while still including its dead load. Results of the FEM rating factors, as well as the other two rating factor approaches, are shown in Figure 2.4.

Overall, the results show that the traditional method produced more conservative rating factors than the NDT and FEM methods. This was especially evident in the interior girders due to the conservative estimates of live load distribution factor as previously discussed. Higher ratings for exterior girders were expected due to larger steel beams. The advanced ratings were able to provide a closer estimation of bridge behavior in its current state due to in-situ load testing which reduced unknowns and verified the FEM. However, the NDT method requires closure of the bridge which could present cost issues and be impractical in some scenarios. The FEM method requires modeling from an engineer experienced in finite element modeling, while still needing to be calibrated based on NDT investigation. There is a trade-off between the relative ease of the methods and the subsequent increase in load rating.

Conclusions from Sanayei et. al. (2015) are described as the following:

- Conventional load rating is faster, easier to use, reviewable, less expensive, and more conservative which promotes safety.
- Conventional load rating with NDT rating adjustment is reviewable, easy to implement, and is more time consuming and costly than conventional load rating.
- FEM load rating is most time consuming, requires modeling experience, lengthier review, but can lead to more accurate results.
- Higher rating factors in the advanced methods were a result of more accurate live load and superimposed deadload distribution factors determined from NDT data.

2.3 Tables

Table 2.1 Experimental and theoretical ultimate strengths for laboratory tested panels (Klaiber et al. 2003).

Panel	Ultimate Strength (kN*m) – Experimental/Theoretical			
	1	2	3	4
Cedar	632/285	662/285	636/285	842/476
Butler	473/362	494/362	334/362	441/362
Black Hawk	521/405[1]	488/405[1]	583/405	549/405

[1] Failure not reached due to loading system limitations; value is midspan moment at maximum applied load

Table 2.2 Condition catalogue of each girder (Mills 2010).

Girder	Test	Condition	Characteristics of Deterioration
1	Flexure	Good	• Longitudinal cracks on the webs extending away from the post-tensioning ducts • Leaching stains visible on webs
2	Flexure	Fair	• Horizontal cracks observed at all ducts • Leaching stains visible on webs
3	Flexure	Poor	• Horizontal cracks observed at all ducts • Surface scaling on east web • Web loss exposing bottom layers of pre-stressing. • Both pre-stressing strands ruptured on west web. • Water leaching stains visible on webs.
4	Shear	Good	• Longitudinal cracks located on the webs extending away from the post-tensioning ducts. • Leaching stains visible on webs.
5	Shear	Poor	• Significant web loss (up to 100 mm.) on east web. • Leaching stains visible on both webs. • Surface scaling on east web. • Outer strand on east web ineffective.
6	Shear	Poor	• Leaching stains visible on webs.

			• Surface scaling on west web. • Exposed strands on one web with moderate level of corrosion.

Table 2.3 Comparison of theoretical and experimental rating factors for girders 1 - 3 at midspan (Mills 2010).

Girder	Values Analyzed	Limit State		HS 20		HSS 30	
				Inventory	Operating	Inventory	Operating
1	Experimental	Strength 1	Pure Bending	2.03	2.63	1.07	1.38
			Flexure-Shear	2.22	2.87	1.40	1.81
	Theoretical	Strength 1	Pure Bending	1.28	1.66	0.81	1.06
			Flexure-Shear	1.35	1.75	0.72	0.93
2	Experimental	Strength 1	Pure Bending	1.82	2.35	0.96	1.24
			Flexure-Shear	2.03	2.63	1.28	1.66
	Theoretical	Strength 1	Pure Bending	1.13	1.46	0.72	0.93
			Flexure-Shear	1.27	1.65	0.68	0.88
3	Experimental	Strength 1	Pure Bending	1.42	1.84	0.75	0.97
			Flexure-Shear	1.67	2.16	1.05	1.36
	Theoretical	Strength 1	Pure Bending	1.01	1.31	0.64	0.83
			Flexure-Shear	1.06	1.37	0.53	0.71

Table 2.4 Rating factors based on Eqs. (1) - (7) for the girder in as built and cracked conditions (Gunasekaran et al. 2023).

Rating Factor	Inventory Rating		Operating Rating	
	As built	Cracked	As built	Cracked
Capacity based [Eqs. (1) and (2)]	1.23	0.96	2.05	1.60
Concrete tension [Eq. (3)]	1.72	_	_	_

Concrete compression [Eq. (4)]	6.32	5.73	_	_
Concrete compression [Eq. (5)]	4.29	3.70	_	_
Prestressing steel tension [Eqs. (6) and (7)]	12.59	<0(-0.12)	20.48	**0.82**

Table 2.5 Nondestructive testing rating summary (Sanayei et. al. 2015).

Girder	**Measured strain εT (με)**	**Theoretical strain ε_c (με)**	**K_a**	**T/W**	**Kb**	**K**	**Nondestructive inventory RF**
G1	91.10	99.30	0.09	0.51	0.8	1.07	4.38
G2	104.4	172.2	0.65	0.53	0.8	1.52	3.71
G3	100.5	172.2	0.71	0.53	0.8	1.57	3.83
G4	103.5	172.2	0.66	0.53	0.8	1.53	3.67
G5	98.50	172.2	0.75	0.53	0.8	1.60	3.84
G6	75.30	28.90	-0.62	0.15	0.0	1.00	3.78

2.4 Figures

Figure 2.1 Typical PCB deterioration (Klaiber et al. 2003).

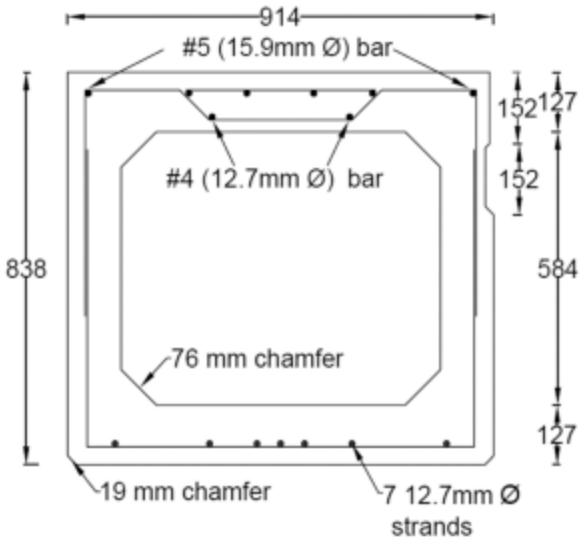

Figure 2.2 Schematic sketch of the cross-section (Gunasekaran et al. 2023).

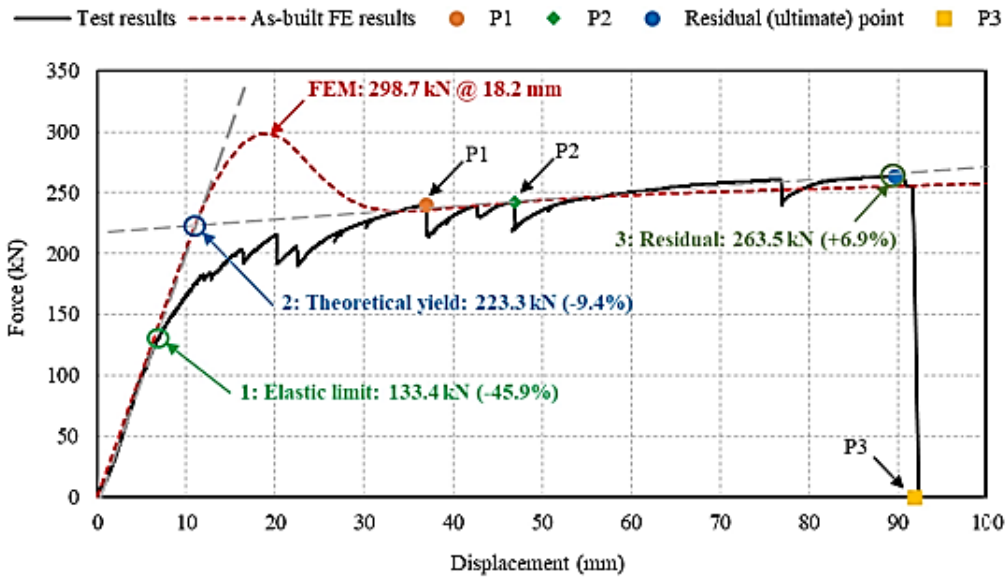

Figure 2.3 Load-deflection behavior of the tested damaged girder versus the numerical as-built behavior of the girder (Gunasekaran et al. 2022).

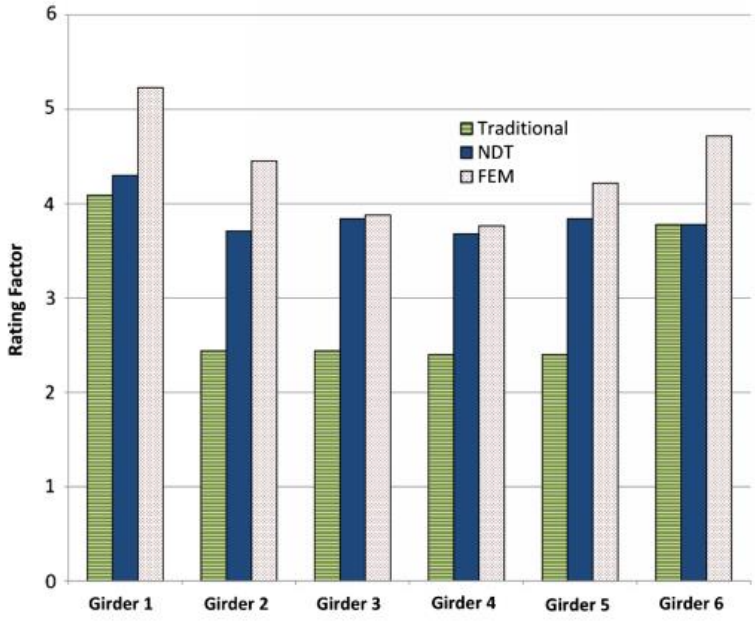

Figure 2.4 Load rating factor comparison (Sanayei et al. 2015).

2.5 Sources

Gunter, Robert Steven, "Structural Evaluation of SCDOT Prestressed Channel Bridges" (2016). *All Theses*. 2570. https://tigerprints.clemson.edu/all_theses/2570

Gunasekaran, D., Mirdad, M. A., & Andrawes, B. (2023). Capacity and load rating of in-service precast prestressed concrete bridge deck girders with transverse cracks. *Journal of Performance of Constructed Facilities*, *37*(2). https://doi.org/10.1061/jpcfev.cfeng-4261

Ingersoll, J. & Wipf, Terry & Klaiber, Fred. (2003). *Experimental Evaluation of Precast Channel Bridges*. https://www.researchgate.net/publication/251344280_Experimental_Evaluation_of_Precast_Channel_Bridges

Mills, B. J. (2010). An autopsical examination of 40 year old pre-tensioned concrete channel girders. *U of Manitoba, M Mech Eng Thesis. MSpace*, https://mspace.lib.umanitoba.ca/handle/1993/21638

Sanayei, Masoud & Ford, Alexandra & Brenner, Brian & Imbaro, Rosalind. (2015). Load Rating of a Fully Instrumented Bridge: Comparison of LRFR Approaches. Journal of Performance of Constructed Facilities. 30. 04015019. 10.1061/(ASCE)CF.1943-5509.0000752.

CHAPTER 3
METHODOLOGY

3.1 Specimen Properties

Skinny leg channel girders are a subset classification of a superstructure type utilizing the beneficial properties of a "C" shape with two legs (webs) cast with a single flange, similar to a double-T section. All channel specimens were originally used in 30-ft. span bridges that were constructed in the 1950's and 1960's, then removed and stored in SCDOT facilities after their roughly 30 – 40 year service life. Dimensions and reinforcement details of the channel section are displayed in Figure 3.1. All material properties listed in the remainder of this paragraph were obtained from and specified in SCDOT drawings and will be referred to from this point forward as "specified properties". Longitudinal reinforcement in the compressive region consisted of No. 3 rebar spaced evenly along the flange width, as well as 10 – 3/8 in. diameter 7-wire strands vertically spaced 1.5 in. on center. The top four strands in each leg were draped downward at midspan while the singular bottom strand in each leg was not, as depicted in Figure 3.1. The four top strands were prestressed with 13,450 lb. of force at release, while the bottom strand was prestressed with 14,000 lb. at release for each leg. Transverse reinforcement in the flange consisted of No. 4 bars spaced 12 in. on center near midspan. Shear reinforcement consisted of No. 4 "U" shaped stirrups spaced 12 in. on center near midspan.

Compressive strength of concrete was f'_c = 5,000 psi. Yield stress for all

mild steel bars consisted of f_y = 40,000 psi. Ultimate stress for all steel prestressed strands consisted of f_{pu} = 250,000 psi. Some channels contained end diaphragms at each end of their length while some did not. Due to limiting scope, it is unclear the exact differences between the girders with and without end diaphragms. However, it is understood that all dimensions of both types of girders are consistent with Figure 3.1. The channels were designed to resist HS-15 truck loading. A copy of typical SCDOT plan set is located in Appendix A.

3.2 Prestressed Concrete Theory Procedure

Nominal moment capacity of the channel girders was calculated in accordance with AASHTO LRFD Bridge Design Specifications (AASHTO 2012). All material properties and dimensions used in the nominal moment capacity calculations were obtained from SCDOT drawings of skinny leg channel girders. Calculations for the nominal moment capacity are displayed in Appendix B.

3.3 Channel Inspection Procedure

All channel girders were inspected for existing deterioration prior to testing. Deterioration was mapped and logged for each channel, which was used to help determine the relationship between experimental girder capacity and existing deterioration. Channel condition was categorized based on the Federal Highway Administration (FHWA) Specifications for the National Bridge Inventory (NBI) inspection criteria (Federal Highway Administration 2022). A condition ranking of 1 - 9 was given to each channel based on observed deterioration. A condition factor (ϕ_c) was assigned to each girder, based on the inspection condition ranking, which will be utilized in the load rating procedure.

3.4 Flexural Test Setup

A total of 13 channels were tested at full scale for flexural resistance in the laboratory. All channel tests utilized the same test setup depicted in Figure 3.2. Total span length from centerline of bearings is 27 ft., with 1.5 ft. of overhang at each end. This was done to eliminate uneven bearing issues due to some channel missing concrete at the ends of their 30 ft. lengths. Both bearing locations created a simply supported bearing condition which employed neoprene bearing pads to level the channel and reduce friction. Two structural steel members, resting on neoprene bearing pads on top of the channel surface, support a stiffened "W" shaped structural steel spreader beam to create a 4-point bending configuration. To ensure proper transfer of load into the prestressed strands, the bearing pads used to support both structural steel members were placed directly in line with each leg. A hydraulic actuator was bolted to a steel frame reaction stand to adequately apply load with minimum individual deflection of the actuator. Pictures of the test setup can be observed in Figure 3.3.

3.5 Data Collection

A 250-kip load cell was used to record applied load in conjunction with an in-line actuator pressure gauge to verify the load cell measurements. A total of four Micro-measurements string potentiometers were used to measure channel vertical displacement at midspan and quarter span. Four Bridge Diagnostic Incorporated (BDI) ST350 Strain Transducers were placed at midspan to record strains of the outermost fibers at the channel top surface and on the soffit of the legs. An STS-4 Wireless Intelliducer acquisition system was used to record output strain data. A VISHAY Micro-

Measurements Data Acquisition System 7000 and P3 Strain Indicator was used to continuously record load and displacement data during testing.

3.6 Material Properties

Drilled concrete cores were extracted from seven channels and tested for their compressive strength. A total of 20 cylinders were drilled using a core drill and diamond-impregnated drill bit. Concrete cores were obtained in accordance with ASTM C 42/C 42M and ACI 214.4R-03, were capped in accordance with ASTM C 617, and tested in accordance with ASTM C 39/C 39M. However, the dimensions of the concrete core specimens were 2 in. by 4 in., which does not conform with ASTM C 39/C 39M or ACI 214.4R-03. There are varying opinions about the effect of small concrete cores (< 3 in. diameter) and their effect on compressive strength. Multiple studies have been conducted on this subject matter, where one particular experiment observed 2x4 in. cylinders which contained compressive strengths 6% less than 4x8 in. cores on average. Two inch diameter cores are also much more susceptible to greater variability of results (ACI 214.4R-03, 2003). Because of the potential inaccuracy and likelihood that the results may need to be modified, the compressive strength tests are not official results. A summary table is presented in Appendix B Table B.3 for reference.

Steel prestressing strands were removed from seven channels and tested for their tensile ultimate strength at the SCDOT Office of Materials and Research. A total of 14 – 30 in. long prestressing strands were collected with various levels of corrosion and section loss. Strand corrosion was classified using a condition rating of one through four. One corresponds to a strand with no corrosion. Two corresponds to a strand with minimal to almost no corrosion. Three corresponds to a strand with corrosion and minor

section loss. Four corresponds to a strand with corrosion and clear section loss. The purpose of classifying strand condition was to categorize strand strength results to better compare their measured tensile strength. It would be counterintuitive to compare the strength of a corroded strand and non-corroded strand without considering the effect of the corrosion. Strands selected for testing were either the lowest strand or second lowest strand. The lowest strands typically possessed more corrosion than the strands above them.

3.7 Load Rating Procedures

The load rating procedures used in this report are in accordance with AASHTO MBE (AASHTO 2018). Two methods of load rating were considered: Load Factor Rating Method (LFR) and Load and Resistance Factor Rating (LRFR). The LRFR method is used for load rating of modern bridge structures, where the LFR method is an appropriate choice for older bridges (AASHTO 2018). Design load rating was of particular interest because it is a beginning check to determine if a bridge shall be posted or not. If a bridge is rated above 1 at the design level, then it will not be posted and all legal truck configurations which utilize the bridge.

There are two different sub-classes of design level rating, inventory and operating levels. Inventory load rating is associated with a certain reliability that is greater than operating load rating. If the inventory rating is less than one, the operating rating must be checked. If the operating rating factor is less than one, the bridge should be rated for each individual truck specified in the legal load rating (second level evaluation) to determine how the bridge shall be posted. Load rating also incorporates different limit states depending upon numerous factors like superstructure type. The four different limit states

that can be considered for a bridge are Strength, Service, Extreme Event, and Fatigue. Strength is the primary limit state and refers to a bridge component's load, moment, or shear capacity. Service limit state refers to stresses in different parts of a structural component. For concrete components, Strength I and Service III limit states, (both design-level LRFR rating checks) must be investigated according to the AASHTO MBE (AASHTO 2018) and were investigated in this thesis. The general LRFR equation used in the load rating analysis is listed below:

$$RF = \frac{C-(\gamma_{DC})(DC)-(\gamma_{DW})(DW)-(\gamma_P)(P)}{(\gamma_{LL})(LL+IM)} \quad (1)$$

where:

$RF =$ Rating Factor

$C =$ Capacity (LRFD)

$DC =$ Dead load effect due to structural components and attachments

$DW =$ Dead load effect due to wearing surface and utilities

$P =$ Permanent loads other than dead loads

$LL =$ Live load effect

$IM =$ Dynamic load allowance

$\gamma_{DC} =$ LRFD load factor for structural components and attachments

$\gamma_{DW} =$ LRFD load factor for wearing surfaces and utilities

$\gamma_P =$ LRFD load factor for permanent loads other than dead loads = 1.0

$\gamma_{LL} =$ Evaluation live load factor

and for strength limit states:

$$C = \varphi_c \varphi_s \varphi R_n \quad (2)$$

φ_c = Condition factor

φ_s = System factor

φ = LRFD resistance factor

R_n = Nominal member resistance (as inspected)

and for service limit states:

$$C = f_R \tag{3}$$

The LFR method integrates different philosophies in the rating process compared to the LRFR method. Allowable stress design (ASD) philosophy is incorporated in the LFR method, while the LRFD philosophy was used to help develop the LRFR method. The LFR method is based on analyzing multiple loads (factored loads) acting on a structure. Inherent uncertainty in the calculations is addressed by load factors, like the LRFR method, however there is less conservative incorporation of resistance factors to reduce the nominal capacity (AASHTO 2002). The general expression for LFR rating factor is described below in Eq. (4):

$$RF = \frac{C-(A_1)(D)}{(A_2)(L)(1+I)} \tag{4}$$

where:

C = Capacity (ASD)

D = Dead load effect

L = Live load effect

I = Impact factor to be used with the live load effect

A_1 = Factor for dead loads

A_2 = Factor for live loads

The LFR method specifies two sub-classes of design level rating (inventory and operating), of which both serviceability and strength load rating equations are described in the AASHTO MBE. These equations are displayed as Eq. (5) - (9) for inventory rating, and Eq. (10) - (11) for operating rating below:

$$RF_{concrete\ tension} = \frac{6\sqrt{f'_c} - (F_D + F_S + F_P)}{(F_l)} \quad (5)$$

$$RF_{concrete\ compression} = \frac{0.6f'_c - (F_D + F_S + F_P)}{(F_l)} \quad (6)$$

$$RF_{concrete\ compression} = \frac{0.4f'_c - \frac{1}{2}(F_D + F_S + F_P)}{(F_l)} \quad (7)$$

$$RF_{prestress\ steel\ tension} = \frac{0.8f^*_y - \frac{1}{2}(F_D + F_S + F_P)}{(F_l)} \quad (8)$$

$$RF_{flexural\ \&\ shear\ strength} = \frac{\varphi R_n - (1.3D + S)}{2.17L(1+I)} \quad (9)$$

$$RF_{flexural\ \&\ shear\ strength} = \varphi R_n - \frac{(1.3D + S)}{1.3L(1+I)} \quad (10)$$

$$RF_{prestress\ steel\ tension} = \frac{0.9f^*_y - \frac{1}{2}(F_D + F_S + F_P)}{(F_l)} \quad (11)$$

where:

$6\sqrt{f'c}$ = Allowable concrete tensile strength

F_d = Unfactored dead loss stress

F_p = Unfactored stress due to prestress forces after all losses

F_s = Unfactored stress due to secondary prestress forces

F_l = Unfactored live load stress including impact

φR_n = Nominal strength of section

D = Unfactored dead load moment or shear

S = Unfactored prestress secondary moment or shear

L = Unfactored live load moment or shear

f^*_y = Prestressing steel yield stress

I = Impact factor

Both the LRFR and LFR methods utilize a design truck that is configured exactly the same. Respective axle weights of both trucks are the same, and the selected distance between the middle and rear axles was 14 ft. The LRFR method incorporates a design lane load of 0.64 kip/ft., which was considered in the structural analysis for live load effects. The LFR method does not incorporate a design lane load, thereby resulting in different calculated live load effects. Only one line of wheels was considered in the calculations. This is due to the fact that only one line of wheels could fit on one channel at a time. Accurate live load distribution calculations could not be conducted due to the channels being tested individually and not as a system. Various factors can affect live load distribution, like transverse tie rod condition or shear key condition, thereby increasing the variability in the comparison of load rating methods. To reduce variability, live load distribution was assumed to be 0.5. A conservative estimate for impact factor (IM) of 33% was utilized for both LRFR and LFR analyses. For simplification, the middle axle was placed at midspan to inflict a near-worst-case loading scenario. A summary of the loading scenarios for both methods are presented in Appendix A.

3.8 Figures

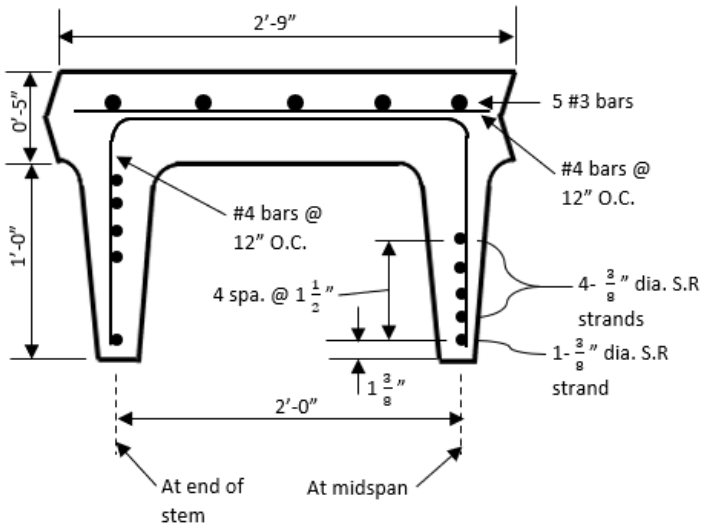

Figure 3.1 Dimensions and reinforcement layout of channels.

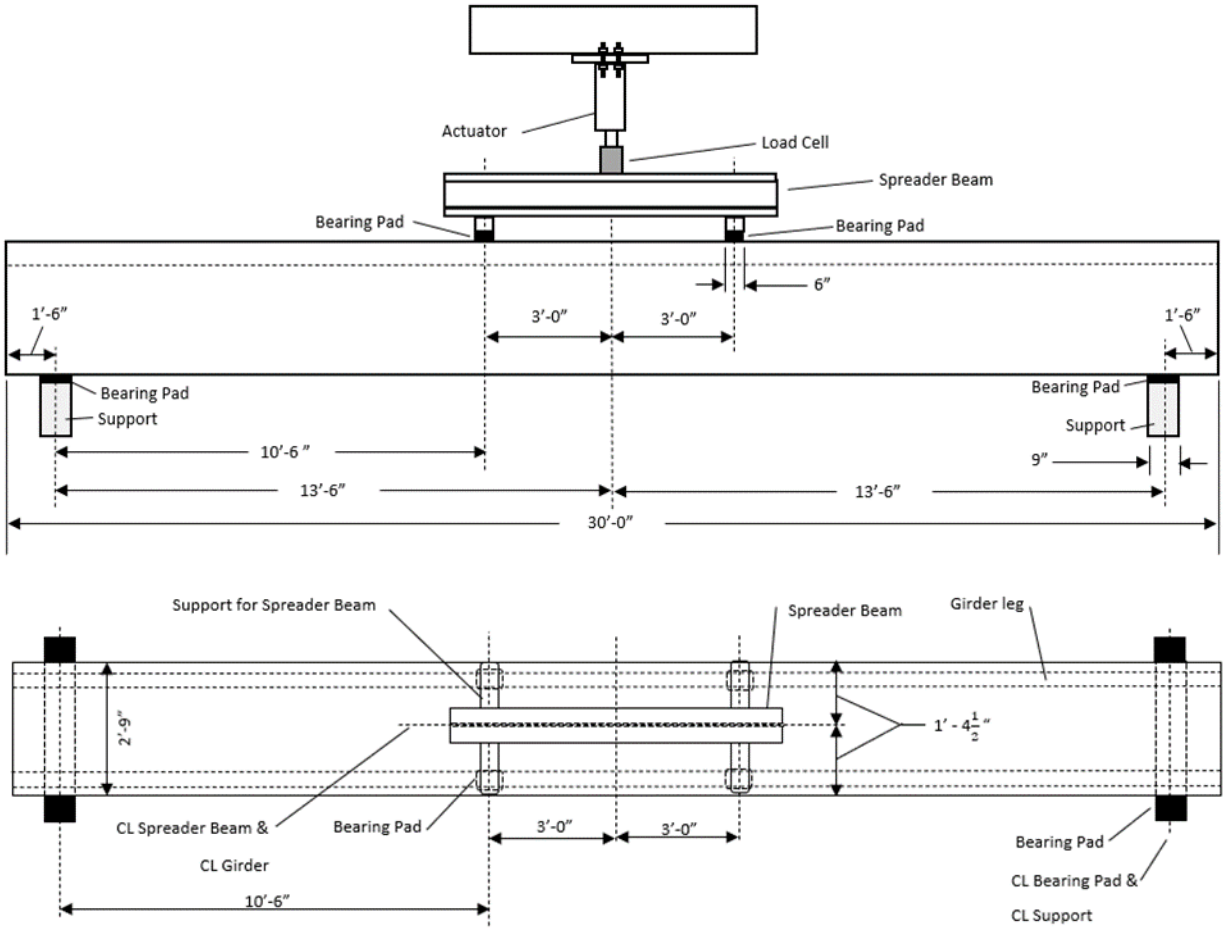

Figure 3.2 Elevation (top) and plan view (bottom) of channel test setup.

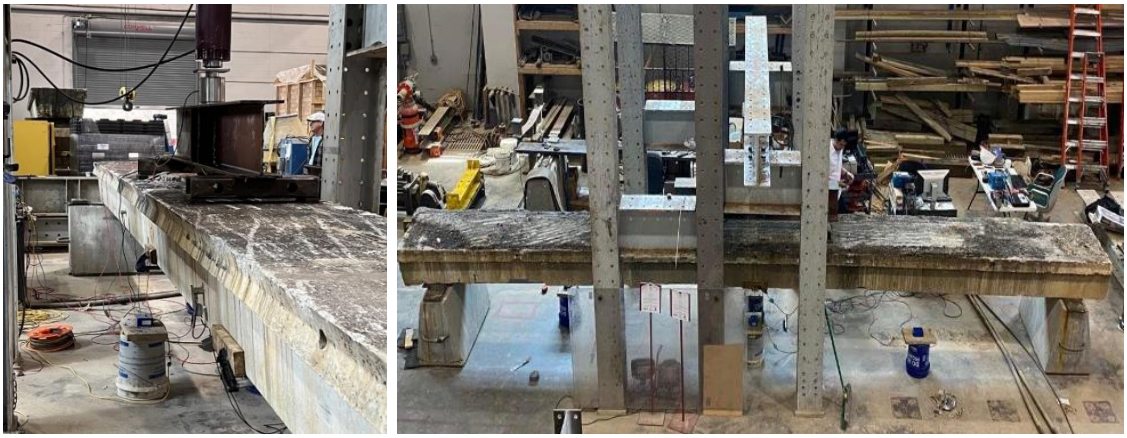

Figure 3.3 Channel test setup

3.9 Sources

AASHTO. 2002. Standard specifications for highway bridges. 17th ed. Washington, DC: AASHTO.

AASHTO. 2012. LRFD bridge design specifications. 6th ed. Washington, DC: AASHTO.

AASHTO. 2018. The manual for bridge evaluation. 3rd ed. Washington, DC: AASHTO.

ACI Committee 214.4R-03. (2003). Guide for Obtaining Cores and Interpreting Compressive Strength Results. Farmington Hills, Michigan. American Concrete Institute.

Federal Highway Administration. (2022). Specifications for the National Bridge Inventory. https://www.fhwa.dot.gov/bridge/snbi/snbi_march_2022_publication.pdf.

CHAPTER 4
RESULTS AND DISCUSSION

4.1 Inspection Results

Initial inspection of each channel prior to testing showed repeating deterioration characteristics that were logged to form a summary of deterioration. These deteriorated state descriptions, as well as their subsequent FWHA NBI condition ratings, are displayed in Table 4.1. All channels with a condition rating of four or below exhibited concrete spalling or cracking that led to several feet of exposed/corroded strand(s). This type of deterioration is considered a major defect that negatively impacted the moment capacity. Some channels had varying levels of strand corrosion due to different factors like length of exposed strand, number of exposed strands, time strands were exposed, cracking or spalling near the clear cover, location the channel was sourced from, and channel end spalling. Figure 4.1 displays the different levels of corrosion, including strands with no corrosion for reference, as a result of the factors previously listed. Deterioration that does not play a significant role in strand corrosion, like flange spalling, is considered less critical and has a lesser effect on the condition rating. Examples of channel deterioration, as described in Table 4.1, can be seen in Figure 4.2. Results of the strand ultimate tensile strength tests are summarized in Table B.1 and B.2 in Appendix B. It is evident that ultimate tensile stresses for strands with condition ratings of a one or two exceed the specified tensile strength of 250 ksi, which contributed to improved flexural

strength of channels compared to the nominal strength. A summary of the concrete compressive tests results are located in Table B.3 in Appendix B. Although the results may be slightly inaccurate due to cylinder size, they also provide additional examples of material properties that were measured well above their nominal values.

4.2 Flexural Test Results

Flexural test results are summarized in Table 4.2. Table 4.2 states the channels as C1, C2, etc., where C1 refers to channel 1 and so on. This naming system will be utilized throughout the remaining chapters. The measured total moment includes moments due to self-weight, wearing surface, and applied load moment. Figure 4.3 displays the moment – deflection behavior of each channel. The behavior of the channels was linear elastic until moment reached roughly 75 kip-ft. Non-linear behavior and continuous reduction in stiffness can be observed after this moment, with no well-defined yield point, which is typical of prestressed concrete beam behavior. Strand yield then rupture in the maximum moment region, coupled with flexural cracking, was observed during testing. The failure modes for the channels consisted of strand yield followed by rupture of the bottom strand or simultaneous rupture of all strands and concrete surface crushing which can be seen in Figure 4.4.

The black solid line in Figure 4.3 demonstrates the LRFD nominal moment capacity. Notice that there is a fairly even split of the moment – deflection data above and below the nominal moment capacity thanks to various levels of deterioration. Also, maximum midspan deflection for channels with moment capacities above the nominal moment capacity are almost double that of channels with moment capacities below the nominal moment capacity. This is true for C1, C2, C3, C7 and C13 which did not have

diaphragms at their ends. It is unclear whether or not the lack of end diaphragms is an indication of enhanced moment capacity and/or maximum deflection. However, the cross-sections and reinforcement of these channels matched those with end diaphragms. C11 also observed total moment capacity higher than the nominal moment capacity (202 kip-ft.) but did not see abnormally large displacement. C11 did contain end diaphragms.

Moment capacities ranged from a maximum 252 kip-ft. to a minimum 97.1 kip-ft. Both the maximum and minimum moment capacities also contained the highest and lowest condition rating of nine and one, respectfully. This makes sense considering the condition rating is influenced by the condition of the strands which also influences moment capacity. The minimum moment capacity from C6 is considered an outlier in the data due to its extreme deteriorated state, and does not fit well with the rest of the channel capacities. Average total moment capacity, not including C6, is 202 kip-ft. which is a 6% increase compared to the nominal moment capacity.

There are at least two explanations as to why some moment capacities are higher than the nominal moment capacity. Actual material properties of the channels were higher than the specified properties from SCDOT drawings. This idea is reinforced by the material strengths observed in Tables B.1, B.2, and B.3. Also, channels without end diaphragms may have been designed with different specified material properties than ones with end diaphragms. This was not proven for all channels without end diaphragms, and there were no SCDOT drawings to confirm this theory. As previously stated, the channels without end diaphragms matched the cross-sectional dimensions, strand diameter, and number of strands in the channels with end diaphragms, which was proven

in the laboratory. Regardless of the reason, moment capacity is higher than the nominal moment capacity unless accumulated deterioration results in capacity reduction.

Figure 4.5 conveys the relationship between moment capacity of each channel and their subsequent FHWA NBI condition rating. There is a very obvious split in the data above and below the black solid line, which indicates nominal moment capacity. All moment capacities that fall below the nominal moment capacity line have a condition rating of four or less. All moment capacities that are above the nominal moment capacity line have condition ratings of six or greater. Figure 4.5 shows that in order to reduce moment capacity below nominal moment capacity, the channel must have a deteriorated state corresponding to a condition factor of four or less. Following the trend in Figure 4.5, one can reasonably assume that a condition factor of five would not reduce the total moment capacity below nominal and therefore justifies the applicability of the FHWA NBI condition rating on this type of superstructure. The average moment capacity of channels with condition ratings being four or lower is 175 kip-ft., which is 8% lower than the nominal moment capacity. The average total moment capacity of channels with condition ratings being six or greater is 230 kip-ft., which is 20% greater than the nominal moment capacity.

4.3 Load Rating Results

Load rating analyses, using LFR and LRFR methodologies, were conducted at the design level for inventory strength and service limit states. The purpose of the load rating analyses was not to determine if the channels would rate sufficiently for HS-20 or HL-93 loading configurations (RF > 1), but rather to determine which method yielded increased load rating compared to each other and to determine how the ratings compared to their

subsequent nominal load ratings. A complete load rating analysis per the AASHTO MBE was not possible and the rating factors presented in this section do not represent a true load rating if these channels were part of a bridge in operation. For the LFR service limit state, only the rating procedure for tensile concrete stresses was checked (Eq. (5)).

The nominal capacity calculated for the strength limit state LFR and LRFR rating factors (191 kip-ft.), which utilized the specified properties obtained from SCDOT documents, was accomplished using LRFD philosophy from the AASHTO MBE. Instead of using ASD philosophy for the inventory strength LFR capacity (C), LRFD was used to preserve a more accurate comparison of both rating methods and comparison of theoretical to experimental results. The LRFD resistance factor (φ) was not included in the nominal rating factor calculations because the nominal capacity is a better comparison to the experimental total moment capacity. In other words, there is no φ factor in the experimental total moment capacity because it is empirical data, meaning φ should be excluded from the inventory strength nominal capacity to eliminate redundancy.

The associated φ_c values for each channel, based on FHWA NBI condition ratings, can be found in Table 4.2. In the Strength I LRFR load rating, φ_c was not considered in Eq. (2) to determine capacity for all channels. There is no need to incorporate φ_c because moment capacities already represent the deteriorated condition and were measured. However, the nominal rating factor calculations utilize appropriate φ_c values to follow AASHTO MBE procedure. This is evident in Tables 4.3 and 4.4, where it is clear that φ_c and φ_s are not used for all the channels and are used for both nominal rating factor calculations.

Table 4.3 displays the results of the LRFR Strength I load rating of channels with good or satisfactory condition. For the nominal rating factor, φ_c =1.00 was used to satisfy the theoretical condition. The analysis shows that all channels in good or satisfactory condition rated higher than the nominal rating factor. Ranges of percent increase in rating factor compared to nominal rating factor are between 37.4% and 6.7%. Thus, all rating factors for channels ranked as 6 – 9 on the FHWA NBI condition rating scale increased when compared to the nominal rating factor. Table 4.4 shows the same concept as Table 4.3, except the analysis was completed on channels in poor condition. φ_c was equal to 0.85 to match the theoretical condition for the nominal rating factor. With the exception of C6, all channels rated higher than the nominal rating factor. Ranges of percent increase in rating factor compared to nominal rating factor are from 15.4% to 1%. The Strength I load rating results are charted in Figure 4.6 to demonstrate that rating factor for each channel exceeds the nominal rating factor of their corresponding φ_c value.

Table 4.5 establishes the results of the LFR Strength load rating for all channels. Results show that channels with condition ratings below four proved to have rating factors less than the nominal rating factor which is expected. This can be seen in Figure 4.7. Because there is no φ_c considered in the LFR nominal capacity, as noted in Eq. (4), all rating factors can only be compared to one nominal rating factor. As a result, increases in rating factor compared to nominal rating factor vary depending on whether or not the moment capacity is greater or less than the nominal moment capacity. If moment capacity is below the nominal moment capacity, then decreases in rating factor are evident and vice versa. This leads to a rating factor that is less likely to increase due to a lack of nominal moment capacity reduction based on deterioration. Also, all strength

rating factors calculated from the LFR method were greater than those calculated from the LRFR method, mainly because of the added live load moment from the lane load in the LRFR method.

The service limit state was investigated for concrete tensile stresses calculated using Eqs. (1) and (3) for LRFR Service III inventory rating factors and Eq. (5) for LFR Service inventory rating factors. All calculations completed in this analysis are based on nominal stress capacity derived from specified properties. Prestressing forces after losses were contributed to the allowable tensile stress, where losses were estimated using the approximate method from the AASHTO LRFD Specifications. No flexural test data was utilized in this procedure. The purpose of this analysis was to determine the effect that varying material properties would have on LRFR and LFR service rating factors. Concrete compressive strength was iterated, starting with f'_c = 5,000 psi and ending with f'_c = 10,000 psi. Concrete compressive strength was varied to represent the potential compressive strengths that could be achieved due to conservative design strengths and full cure time, and to estimate the rating factor for results similar to those of Table B.3. Results from this analysis are displayed in Tables 4.6 and 4.7, as well as Figure 4.8. The LRFR service analysis resulted in lower rating factors compared to the LFR service analysis. This is mainly due to the LRFR lane load which produces higher live load stress. Both method rating factor increased by 23% as compressive strength was increased from f'_c = 5,000 psi to f'_c = 10,000 psi.

4.4 Tables

Table 4.1 Summary of channel deteriorated state.

Channel	FHWA NBI Condition Rating	Description
C1	7	• Localized spalling at one channel end exposing strands. • Localized flange spalling. • "Some minor defects".
C2	9	• Localized spalling on soffit of leg. • Localized inherent flange deterioration. • "Isolated inherent defects".
C3	7	• Localized spalling at one channel end exposing strands. • Some flange spalling. • "Some minor defects".
C4	4	• Localized spalling at one channel end exposing one strand. • Some diaphragm spalling. • Three feet of one strand exposed and corroded. • "Isolated major defect".
C5	3	• Some diaphragm spalling. Some leg spalling. • Several feet of one exposed strand with corrosion at two different locations in flexural/shear zone. • "Major defects; performance seriously affected".
C6	1	• Extreme spalling and missing concrete near midspan. Large cracks at this location. • All five strands on one leg exposed and corroded. • "Major defects; imminent Failure".
C7	6	• Widespread flange spalling. • Widespread leg spalling. • Some diaphragm spalling. • "Widespread minor defects".
C8	3	• Some leg spalling. • Several feet of one exposed strand with corrosion at two different locations in flexural/shear zone. • Isolated large crack on soffit of leg. • "Major defects; performance seriously affected".
C9	3	• Widespread flange spalling. • Several feet of exposed strand with corrosion at two different locations in flexural/shear zone. • Some large cracks on exterior side of legs. • "Major defects; performance seriously affected".
C10	2	• Isolated web spalling.

		• Several feet of exposed strand with corrosion at multiple locations. • Rust stains and spalling of concrete along 75% of one leg soffit.
C11	6	• Widespread flange spalling. • Some leg spalling. • Isolated moderate leg spalling defect. • “Widespread minor and isolated moderate defects”.
C12	4	• Widespread very large cracks at or near soffit of legs with rust stains. • Some leg spalling. • Some flange spalling and isolated diaphragm spalling. • Widespread moderate defects; strength is affected”.
C13	7	• Some flange spalling. • Isolated spalling on interior of leg. • “Some minor defects”.

Table 4.2 Summary of flexural test results.

Channel	Asphalt Depth (in.)	Contains Diaphragm	M_1 (kip-ft.)	M_2 (kip-ft.)	M_3 (kip-ft.)	P_3 (kip)	D_3 (in.)	M_3/M_n	NBI Condition	NBI Rating	φ_c
C1	0	No	22.3	0.0	245	40.7	10.2	1.28	Good	7	1.00
C2	0	No	22.3	0.0	252	42.4	14.5	1.32	Excellent	9	1.00
C3	0	No	22.3	0.0	244	41.1	10.5	1.28	Good	7	1.00
C4	0	Yes	22.3	0.0	183	28.2	7.70	0.958	Poor	4	0.85
C5	0	Yes	22.3	0.0	165	25.5	3.40	0.864	Serious	3	0.85
C6	0	Yes	22.3	0.0	97.1	13.4	4.30	0.508	IF	1	0.85
C7	0	No	22.3	0.0	209	44.0	3.70	1.09	Satisfactory	6	1.00
C8	2	Yes	22.3	5.5	172	27.5	4.40	0.901	Serious	3	0.85
C9	2	Yes	22.3	4.6	184	29.0	4.40	0.963	Serious	3	0.85
C10	0	Yes	22.3	0.0	166	26.6	3.30	0.869	Critical	2	0.85
C11	0	Yes	22.3	0.0	202	34.0	5.00	1.06	Satisfactory	6	0.95
C12	0	Yes	22.3	0.0	177	29.0	6.60	0.927	Poor	4	0.85
C13	0	No	22.3	0.0	227	39.0	11.0	1.19	Good	7	1.00

Notes:
C1-C7 tested at Clemson University (CU). C8-C13 tested at University of South Carolina (USC)
C1-C7 (CU) were sourced from Fork Shoals lot; C8-C13 (USC) were sourced from Saluda Yard lot
M_1: Dead load moment
M_2: Wearing surface moment
M_3: Peak total measured moment (capacity)
P_3: Peak applied load
D_3: Deflection at peak applied load
M_n = 191 kip-ft. (nominal moment capacity)
IF: Imminent Failure
All test setups utilized a moment arm (Figure 3.2) of 10.5 ft., except for C4 (10 ft.)
Condition and Rating derived from FHWA NBI
φ_c based on NBI condition rating per AASHTO MBE

Table 4.3 LRFR Strength I (inventory) design load rating (good/satisfactory condition).

	Mn (ft-kips)	φ_c	φ_s	C (ft-kips)	γ_{DC}	DC (ft-kips)	γ_{DW}	DW (ft-kips)	γ_{LL}	LL (ft-kips)	IM	Rating Factor	% Increase
Nominal	*191*	*1.00*	*1.00*	*191*	*1.25*	*22.3*	*1.50*	*0*	*1.75*	*101*	*1.33*	*0.761*	*NA*
C1	245	NA	NA	245	1.25	22.3	1.50	0	1.75	*101*	1.33	1.01	33.1%
C2	252	NA	NA	252	1.25	22.3	1.50	0	1.75	*101*	1.33	1.05	37.4%
C3	244	NA	NA	244	1.25	22.3	1.50	0	1.75	*101*	1.33	1.01	32.5%
C7	209	NA	NA	209	1.25	22.3	1.50	0	1.75	*101*	1.33	0.845	11.0%
C11	202	NA	NA	202	1.25	22.3	1.50	0	1.75	*101*	1.33	0.813	6.70%
C13	227	NA	NA	227	1.25	22.3	1.50	0	1.75	*101*	1.33	0.929	22.1%

Table 4.4 LRFR Strength I (inventory) design load rating (poor condition).

	Mn (ft-kips)	**φ_c**	**φ_s**	**C (ft-kips)**	**γ_{DC}**	**DC (ft-kips)**	**γ_{DW}**	**DW (ft-kips)**	**γ_{LL}**	**LL (ft-kips)**	**IM**	**Rating Factor**	**% Increase**
Nominal	*191*	*0.85*	*1.00*	*162*	*1.25*	*22.3*	*1.50*	*0.0*	*1.75*	*101*	*1.33*	*0.628*	*NA*
C4	183	NA	NA	183	1.25	22.3	1.50	0.0	1.75	*101*	1.33	0.724	15.4%
C5	165	NA	NA	165	1.25	22.3	1.50	0.0	1.75	*101*	1.33	0.640	2.00%
C6	97.1	NA	NA	97.1	1.25	22.3	1.50	0.0	1.75	*101*	1.33	0.323	-48.5%
C8	172	NA	NA	172	1.25	22.3	1.50	5.5	1.75	*101*	1.33	0.634	1.00%
C9	184	NA	NA	184	1.25	22.3	1.50	4.6	1.75	*101*	1.33	0.696	11.0%
C10	166	NA	NA	166	1.25	22.3	1.50	0.0	1.75	*101*	1.33	0.645	2.70%
C12	177	NA	NA	177	1.25	22.3	1.50	0.0	1.75	*101*	1.33	0.696	10.9%

Table 4.5 LFR Strength (inventory) design load rating.

	C (ft-kips)	**A1**	**D (ft-kips)**	**A2**	**LL (ft-kips)**	**I**	**Rating Factor**	**% Increase**
Nominal	*191*	*1.3*	*22.3*	*2.17*	*65*	*0.33*	*0.864*	*NA*
C1	245	1.3	22.3	2.17	65	0.33	1.15	33.3%
C2	252	1.3	22.3	2.17	65	0.33	1.19	37.7%
C3	244	1.3	22.3	2.17	65	0.33	1.15	32.7%
C4	183	1.3	22.3	2.17	65	0.33	0.821	-4.94%
C5	165	1.3	22.3	2.17	65	0.33	0.725	-16.0%
C6	97.1	1.3	22.3	2.17	65	0.33	0.363	-58.0%
C7	209	1.3	22.3	2.17	65	0.33	0.960	11.1%
C8	172	1.3	27.8	2.17	65	0.33	0.724	-16.1%
C9	184	1.3	26.9	2.17	65	0.33	0.794	-8.01%
C10	166	1.3	22.3	2.17	65	0.33	0.730	-15.4%
C11	202	1.3	22.3	2.17	65	0.33	0.922	6.79%
C12	177	1.3	22.3	2.17	65	0.33	0.789	-8.64%
C13	227	1.3	22.3	2.17	65	0.33	1.06	22.2%

Table 4.6 LRFR Service III (inventory) design load rating for tensile concrete stresses.

f'_c (ksi)	C (ksi)	γ_D	DC (ksi)	DW (ksi)	γ_{LL}	LL (ksi)	IM	Rating Factor
5.0	*1.87*	*1.00*	*0.65*	*0*	*0.80*	*2.97*	*1.33*	*0.42*
5.5	*1.91*	*1.00*	*0.65*	*0*	*0.80*	*2.97*	*1.33*	*0.44*
6.0	*1.95*	*1.00*	*0.65*	*0*	*0.80*	*2.97*	*1.33*	*0.45*
6.5	*1.98*	*1.00*	*0.65*	*0*	*0.80*	*2.97*	*1.33*	*0.46*
7.0	*2.01*	*1.00*	*0.65*	*0*	*0.80*	*2.97*	*1.33*	*0.47*
7.5	*2.04*	*1.00*	*0.65*	*0*	*0.80*	*2.97*	*1.33*	*0.48*
8.0	*2.06*	*1.00*	*0.65*	*0*	*0.80*	*2.97*	*1.33*	*0.49*
8.5	*2.09*	*1.00*	*0.65*	*0*	*0.80*	*2.97*	*1.33*	*0.50*
9.0	*2.11*	*1.00*	*0.65*	*0*	*0.80*	*2.97*	*1.33*	*0.51*
9.5	*2.13*	*1.00*	*0.65*	*0*	*0.80*	*2.97*	*1.33*	*0.51*
10.	*2.15*	*1.00*	*0.65*	*0*	*0.80*	*2.97*	*1.33*	*0.52*

Table 4.7 LFR Service (inventory) design load rating for tensile concrete stresses

f'_c (ksi)	$6\sqrt{f'_c}$	F_d (ksi)	F_p (ksi)	F_l (ksi)	Rating Factor
5.0	*0.424*	*0.65*	*1.450*	*2.54*	*0.48*
5.5	*0.445*	*0.65*	*1.467*	*2.54*	*0.50*
6.0	*0.465*	*0.65*	*1.481*	*2.54*	*0.51*
6.5	*0.484*	*0.65*	*1.494*	*2.54*	*0.52*
7.0	*0.502*	*0.65*	*1.505*	*2.54*	*0.53*
7.5	*0.520*	*0.65*	*1.515*	*2.54*	*0.54*
8.0	*0.537*	*0.65*	*1.524*	*2.54*	*0.55*
8.5	*0.553*	*0.65*	*1.532*	*2.54*	*0.56*
9.0	*0.569*	*0.65*	*1.540*	*2.54*	*0.57*
9.5	*0.585*	*0.65*	*1.546*	*2.54*	*0.58*
10.	*0.600*	*0.65*	*1.552*	*2.57*	*0.59*

4.5 Figures

Figure 4.1 Various levels of strand corrosion.

Figure 4.2 Examples of channel deterioration.

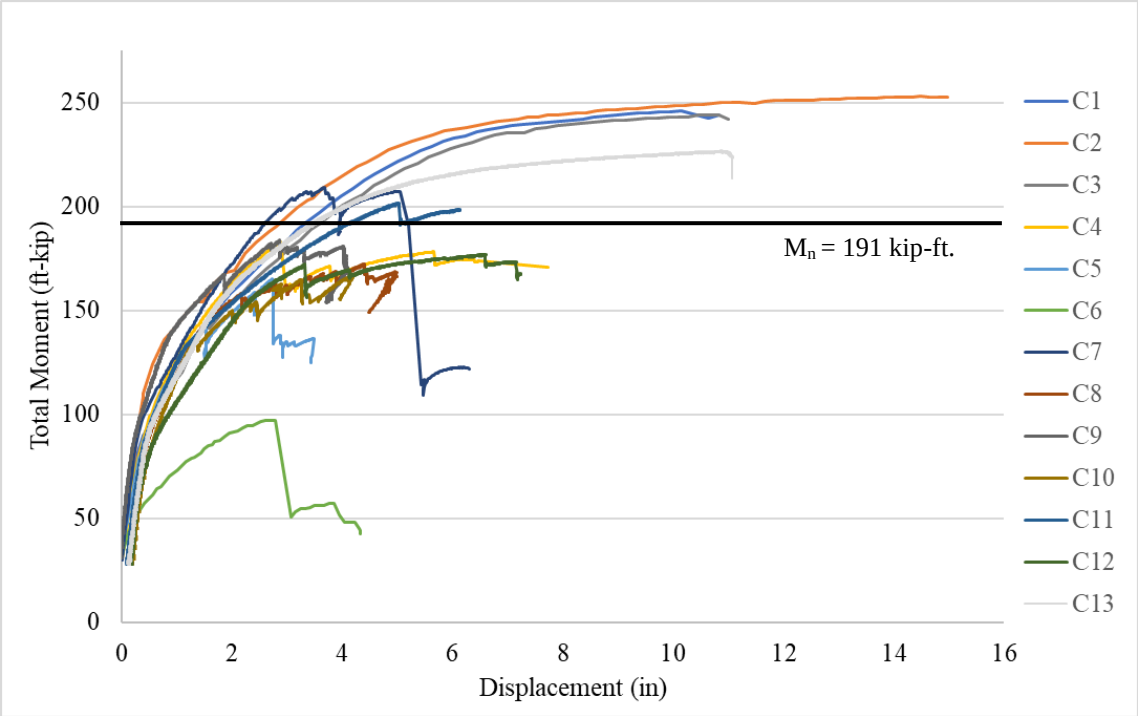

Figure 4.3 Moment vs. displacement.

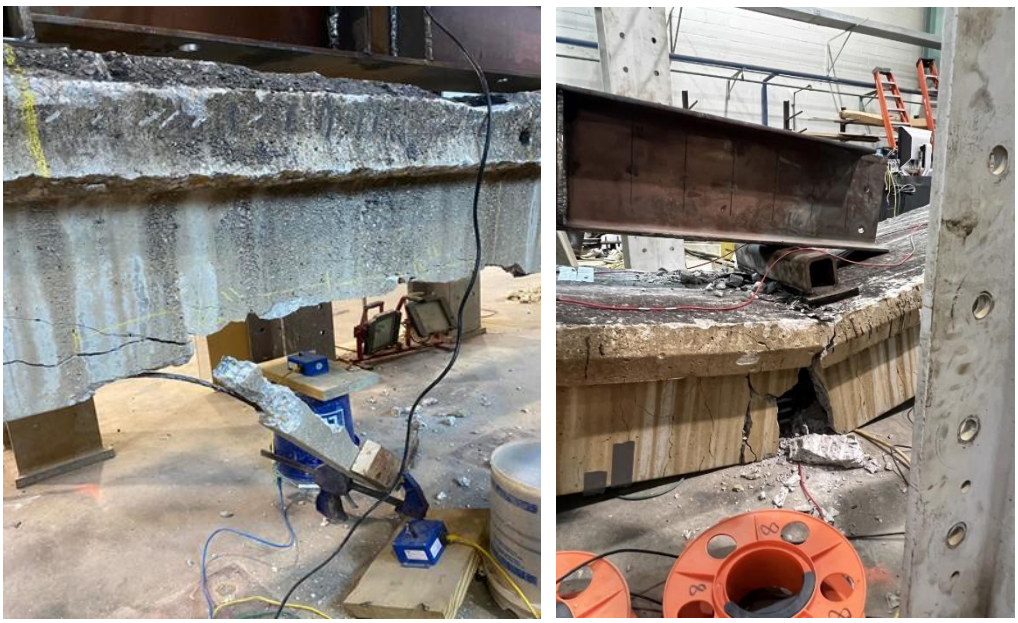

Figure 4.4 Strand rupture (left); and strand rupture coupled with concrete crushing (right).

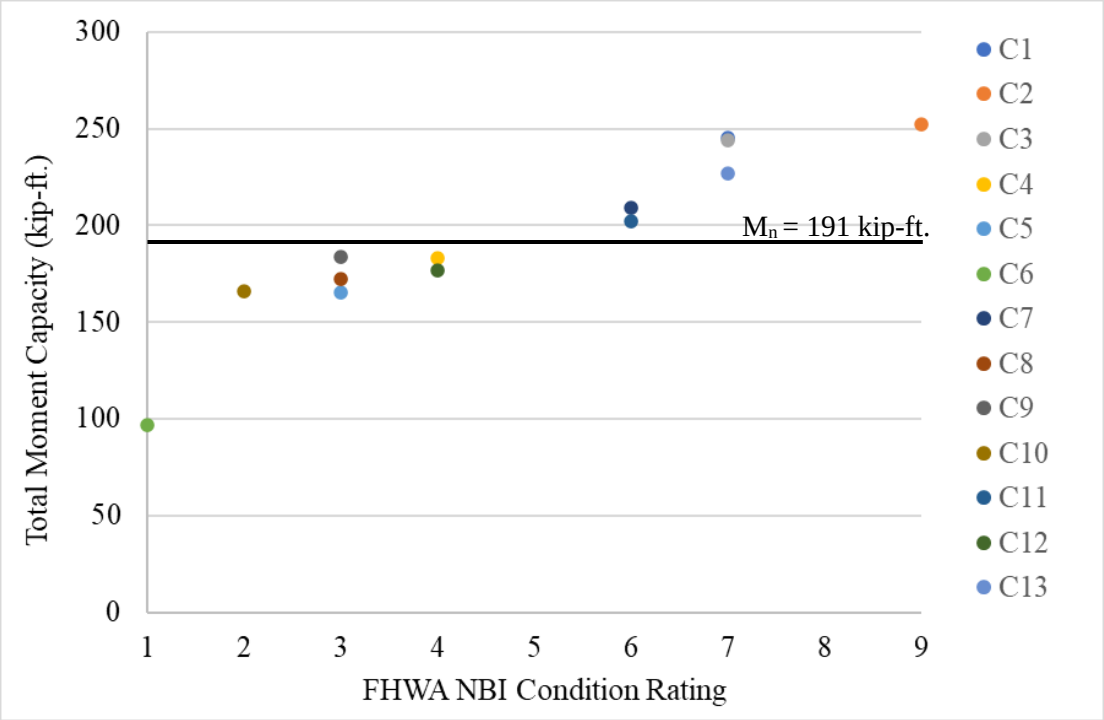

Figure 4.5 Total moment capacity and corresponding condition rating.

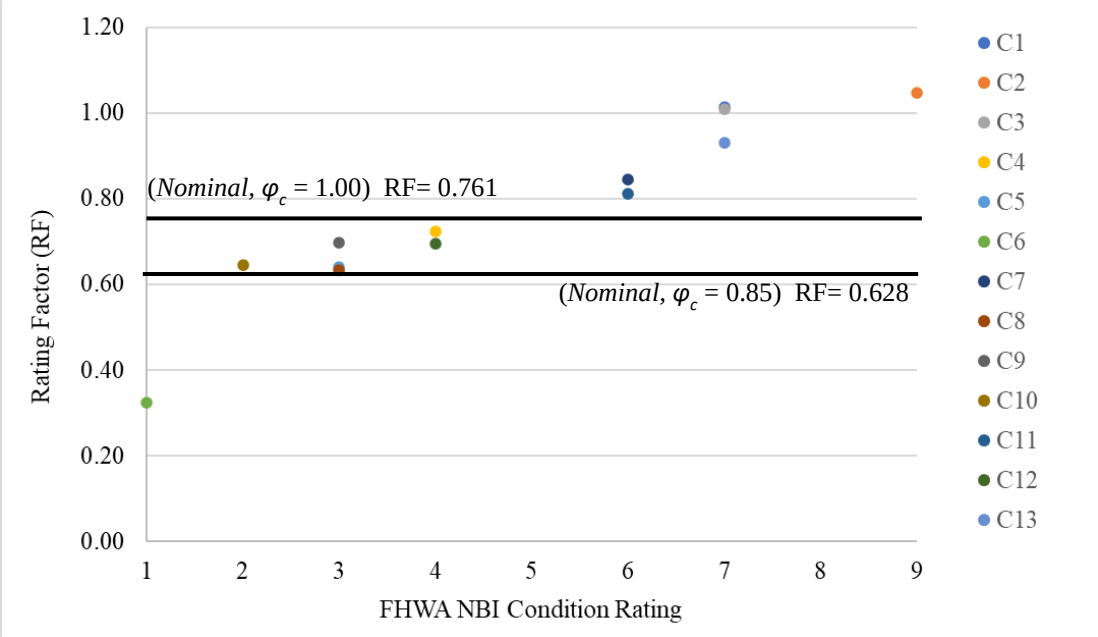

Figure 4.6 LRFR Strength I (inventory) rating factor and corresponding condition rating.

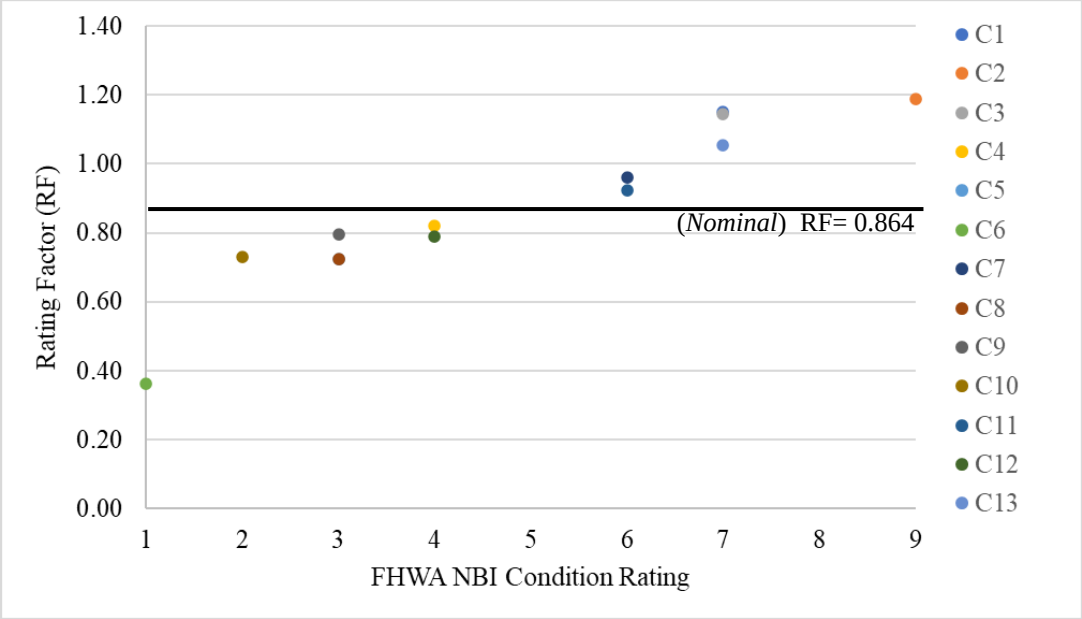

Figure 4.7 LFR Strength (inventory) rating factor and corresponding condition rating.

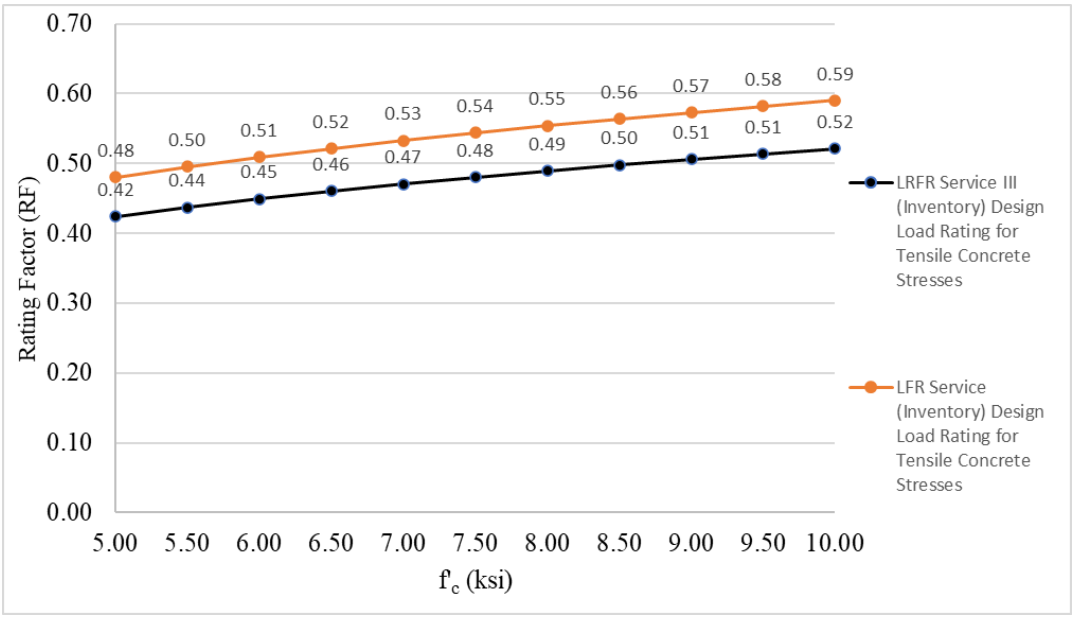

Figure 4.8 Service (inventory) rating factor based on concrete compressive strength.

CHAPTER 5
CONCLUSIONS

5.1 Summary

The primary goal of this thesis is to contribute to the reduction of load restricted bridges in the state of South Carolina. Thirteen prestressed concrete skinny leg channels were obtained from SCDOT facilities, inspected for existing deterioration, and tested at full scale to complete failure. Applied load and midspan deflection were analyzed to understand flexural behavior. Applied load was converted to total moment, in order to determine the capacity of each channel. Capacity was compared with condition rating to determine the deterioration effect on capacity. Capacity was also used to calculate LFR and LRFR rating factors. LFR and LRFR rating factors were compared to each other, and to their subsequent nominal rating factors.

5.2 Conclusions Related to Flexural Capacity

Channels were visually inspected prior to testing to determine any existing deterioration that may lead to reduced flexural capacity. Reoccurring deterioration characteristics that had an impact on flexural capacity were identified and deemed significant based on the FHWA NBI condition rating descriptions. The goals of performing experimental testing were to understand flexural behavior/capacity

and identify their relationships with deterioration. Conclusions are as follows:

- The most significant form of deterioration observed in the channels was concrete cracking or spalling due to several feet of corroded strand(s). Channels that exhibited this deteriorated state received a minimum condition rating of four. The most consistent form of deterioration observed was concrete spalling on the legs or exterior portions of the flange near the shear keys.
- Moment – displacement response was typical of a prestressed concrete beam, where moment capacity corresponded with strand rupture. Channels that did not contain end diaphragms had higher moment capacities and midspan deflections than those that did, regardless of condition rating. No origin for improved performance of channels without end diaphragms was developed.
- All channels with condition ratings six or greater had moment capacities greater than the nominal moment capacity. This is due to material properties measured greater than SCDOT specified properties and the lack of deterioration to reduce capacity.
- All channels with condition ratings four or less had moment capacities less than the nominal moment capacity. Channels containing defects where "strength is affected" were proven to have decreased moment capacities compared to the nominal moment capacity. Therefore, the FHWA NBI inspection method is an acceptable way to anticipate deterioration effects on capacity prior to any testing.

5.3 Conclusions Related to Load Rating

Load rating analysis was conducted using the LRFR and LFR methods described in the AASHTO MBE. Both strength and service limit states were analyzed at the

inventory design level. The design level is an important first step in order to determine if a bridge may be posted or not. The specific goals of the load rating analysis were to compare the two rating methods to see which one yields a higher load rating and compare the nominal load ratings to the experimental load ratings.

- The AASHTO MBE states that for condition ratings of four or less, $\varphi_c = 0.85$ shall be used to reduce the nominal capacity by 15%. C4, C8, C9, C10, and C12 all reported decreases in capacity of 4.2%, 9.9%, 3.7%, 13%, and 7.3% respectively. In this experiment AASHTO MBE guidelines conservatively estimate the effect of deterioration on nominal capacity, which results in a Strength I LRFR nominal load rating that does not accurately portray experimental behavior.
- The LFR method produced greater strength and service rating factors compared to the LRFR method. As a result, the LFR method could be used when evaluating prestressed skinny leg channel girders to help produce the highest rating factors possible.
- By using the moment capacity from the experimental testing of channels, increases in load ratings, when compared to the nominal moment capacity, are achievable due to higher than specified material properties.
- LRFR method proved to produce higher increases in strength rating factor than the LFR method did for channels in poor condition when compared to the nominal rating factor. This is attributed to the difficulty calculating the effects of deterioration on nominal capacity in the LFR method, especially if strand cross-sectional area loss is not visible. It is also attributed to the conservative estimate of deterioration effect on nominal capacity in the LRFR method.

- Service load ratings were very low compared to strength ratings for both methods. This could be attributed to the difficulties calculating the prestressing time dependent losses. Not enough information was available to use the refined estimates of time-dependent losses method. The approximate method was used, but is a conservative estimate which reduces the effective prestressing stress, concrete tensile capacity, and service load ratings.

5.4 Recommendations and Future Work

It can be cumbersome to find the balance between conservativeness and cost-efficiency when load rating older bridges. The main concern with both rating methods lies in their ability to accurately estimate reductions in nominal capacity and estimate improvements in nominal capacity due to enhanced material strengths. Perhaps a new scale for φ_c should be introduced for these types of channels where condition rating of two would correspond to $\varphi_c = 0.85$, condition ratings of 3-4 corresponds to $\varphi_c = 0.90$, and condition rating of 5 corresponds to $\varphi_c = 0.95$. Or, a method could be derived where linear interpolation is utilized based on a more precise condition rating (e.g., 3.75). If the test population is large enough, φ_c values corresponding to condition ratings of 6 or above could be used to increase the nominal capacity to match experimental capacity with acceptable confidence. More research must be completed on prestressed skinny leg channel bridge behavior and appropriate load rating methods to match behavior effectively and safely.

- Studies should be conducted on channel bridges as a structural system. A more in-depth analysis into skinny leg channel bridges as a structural system is required in order to understand how they behave in load distributing configurations.

Improved load distribution may play a vital role in increasing rating factors. Non-destructive testing and finite element modelling could also provide additional analysis tools to dial in a rating factor technique to maximize rating factor.

- Studies should be conducted on channels to determine typical material properties. As indicated in this thesis, material properties are often times higher than specified in drawings due to built-in conservatism. Adjustments to material properties, which will in turn increase capacity, will increase load rating for both the strength and service limit states.
- More studies should be conducted on channel flexural behavior and the relationship with existing deterioration, as well as a modified load rating technique to minimize load postings. A further continuation of this thesis, with more data collected and a further examination of applicable modifications to the LRFR method, will be required to accurately predict deterioration effects on capacity. Specifically, different ways to determine or calculate φ_c must be investigated, as well as a better way to determine nominal capacity reduction in the LFR method that does not rely on visual observation of strand condition.

REFERENCES

AASHTO. 2002. Standard specifications for highway bridges. 17th ed. Washington, DC: AASHTO.

AASHTO. 2012. LRFD bridge design specifications. 6th ed. Washington, DC: AASHTO.

AASHTO. 2018. The manual for bridge evaluation. 3rd ed. Washington, DC: AASHTO.

ACI Committee 214.4R-03. (2003). Guide for Obtaining Cores and Interpreting Compressive Strength Results. Farmington Hills, Michigan. American Concrete Institute.

Alampalli, S., Frangopol, D. M., Grimson, J., Halling, M. W., Kosnik, D. E., Lantsoght, E. O. L., Yang, D., & Zhou, Y. E. (2021). Bridge Load Testing: State-of-The-Practice. Journal of Bridge Engineering, 26(3), [03120002]. https://doi.org/10.1061/(ASCE)BE.1943-5592.0001678

Federal Highway Administration. (2022). Specifications for the National Bridge Inventory. https://www.fhwa.dot.gov/bridge/snbi/snbi_march_2022_publication.pdf

Gunasekaran, D., Mirdad, M. A., & Andrawes, B. (2023). Capacity and load rating of in-service precast prestressed concrete bridge deck girders with transverse cracks. *Journal of Performance of Constructed Facilities, 37*(2). https://doi.org/10.1061/jpcfev.cfeng-4261

Gunter, Robert Steven, "Structural Evaluation of SCDOT Prestressed Channel Bridges" (2016). *All Theses*. 2570. https://tigerprints.clemson.edu/all_theses/2570Ingersoll, J. & Wipf, Terry & Klaiber, Fred. (2003). *Experimental Evaluation of Precast Channel Bridges*. https://www.researchgate.net/publication/251344280_Experimental_Evaluation_of_Precast_Channel_Bridges

Mills, B. J. (2010). An autopsical examination of 40 year old pre-tensioned concrete channel girders. *U of Manitoba, M Mech Eng Thesis. MSpace*, https://mspace.lib.umanitoba.ca/handle/1993/21638

Sanayei, Masoud & Ford, Alexandra & Brenner, Brian & Imbaro, Rosalind. (2015). Load Rating of a Fully Instrumented Bridge: Comparison of LRFR Approaches. Journal of Performance of Constructed Facilities. 30. 04015019. 10.1061/(ASCE)CF.1943-5509.0000752.

South Carolina: ASCE's 2021 infrastructure report card. ASCE's 2021 Infrastructure Report Card |. (2021, September 13). Retrieved February 7, 202.3, from https://infrastructurereportcard.org/state-item/south-carolina/

South Carolina Department of Transportation. (2019). *Transportation Asset Management Plan*. https://www.scdot.org/performance/pdf/reports/TAMP.pdf

South Carolina Department of Transportation. (2019). *Load Rating Guidance Document*. https://www.scdot.org/business/pdf/bridgemaintenance/loadrating/SCDOT-BridgeLoad-RatingGuidance-Doc-NoHigh.pdf.

APPENDIX A: FIGURES

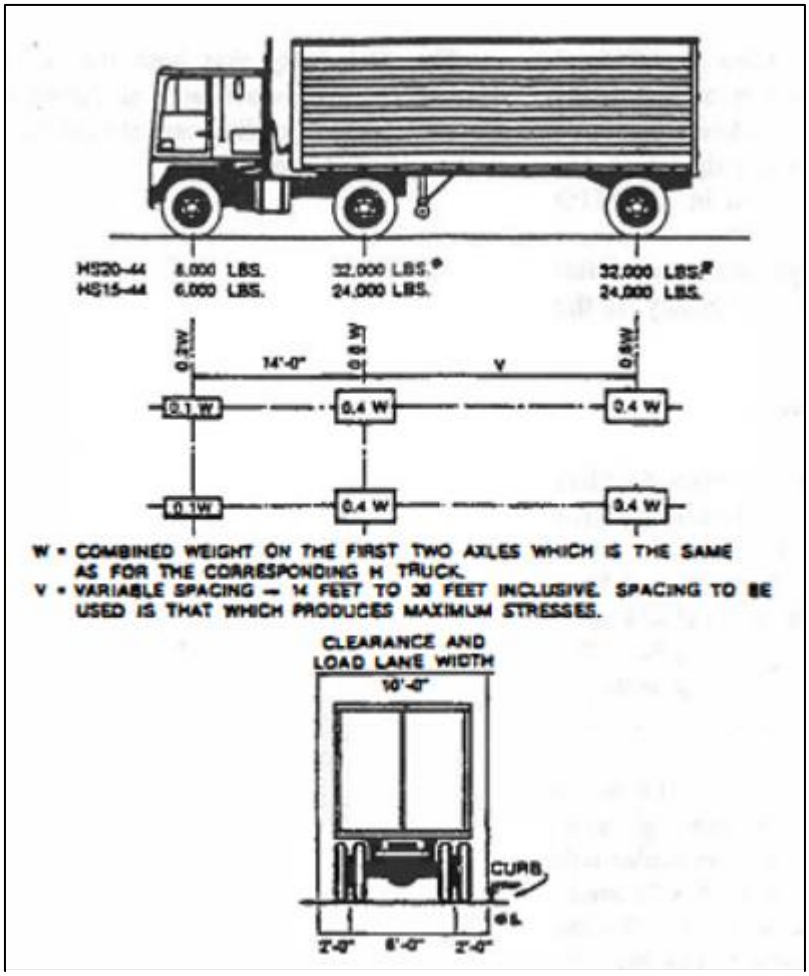

Figure A.1 HS-20 truck configuration (AASHTO 2018).

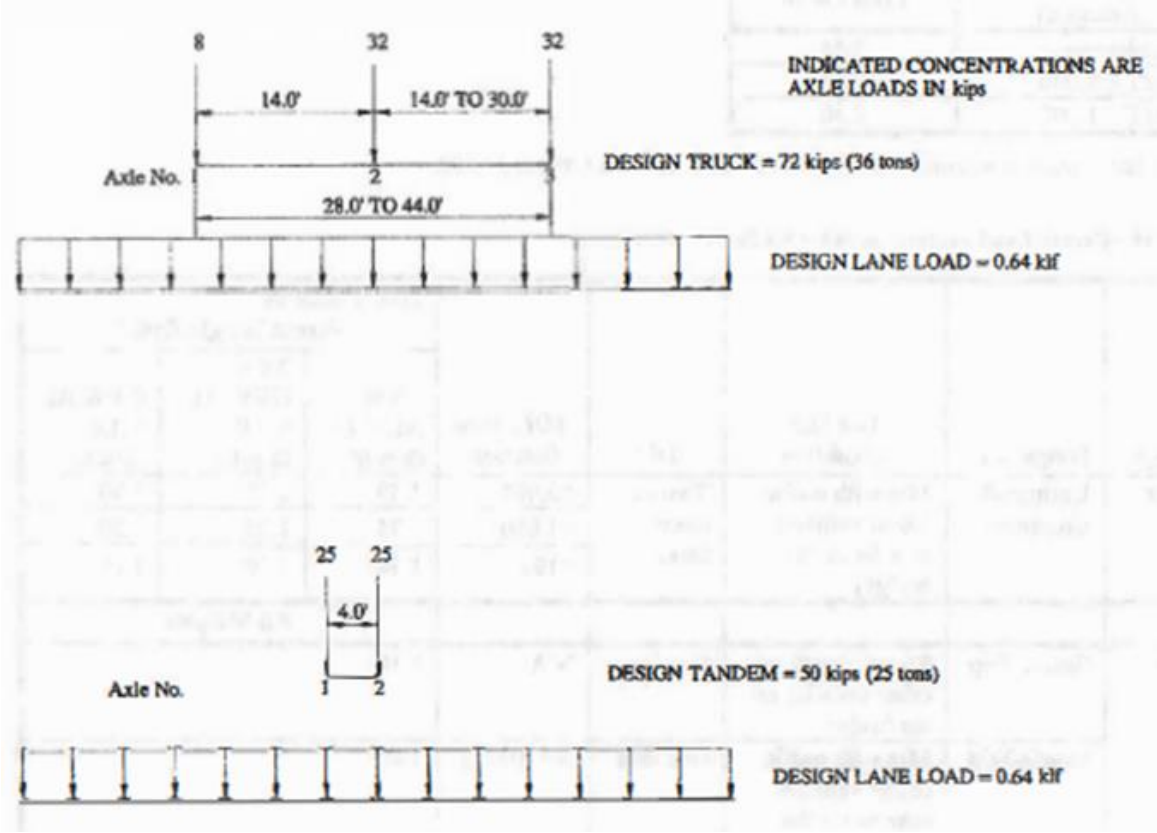

Figure A.2 HL-93 loading scenarios (AASHTO 2018).

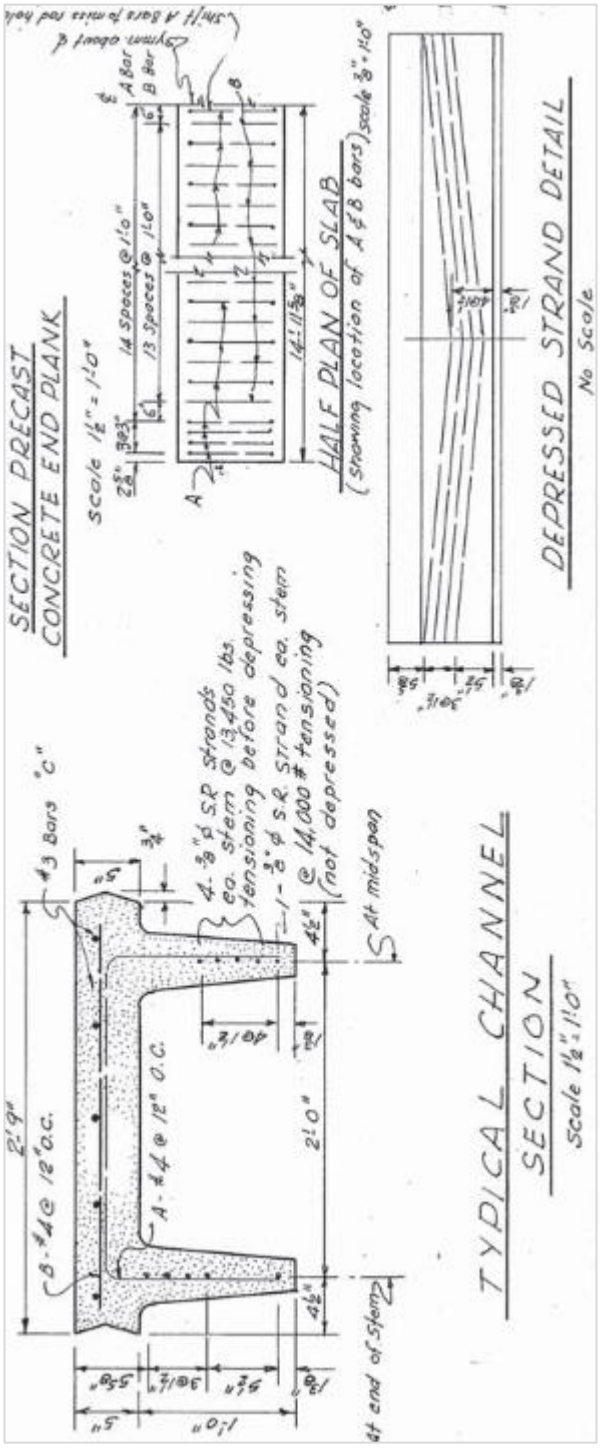

Figure A.3 SCDOT channel sketch.

Figure A.4 C1 (NBI 7) end spalling, minor defect.

Figure A.5 C1 (NBI 7) exposed strand.

Figure A.6 C1(NBI 7) flange spalling, minor defect.

Figure A.7 C2 (NBI 9) end deterioration.

Figure **Error! Use the Home tab to apply 0 to the text that you want to appear here.**A.8 C2 (NBI 9) inherent defect.

Figure A.9 C3 (NBI 7) flange spalling.

Figure A.10 C3 (NBI 7) end spalling.

Figure A.11 C3 (NBI 7) exposed strands.

Figure A.12 C4 (NBI 4) moderate spall.

Figure A.13 C4 (NBI 4) moderate spall and corrosion.

Figure **Error! Use the Home tab to apply 0 to the text that you want to appear here.**A.14 C4 (NBI 4) major defect near quarter span.

Figure A.15 C5 (NBI 3) large spalling, moderate defect.

Figure A.16 C5 (NBI 3) major defect near load point.

Figure A.17 C5 (NBI 3) major defect.

Figure A.18 C6 (NBI 1) imminent failure at midspan.

Figure A.19 C6 (NBI 1) severe deterioration.

Figure A.20 C7 (NBI 6) widespread minor defects.

Figure A.21 C7 (NBI 6) flange spalling.

Figure A.22 C8 (NBI 3) major defect.

Figure A.23 C8 (NBI 3) moderate spall.

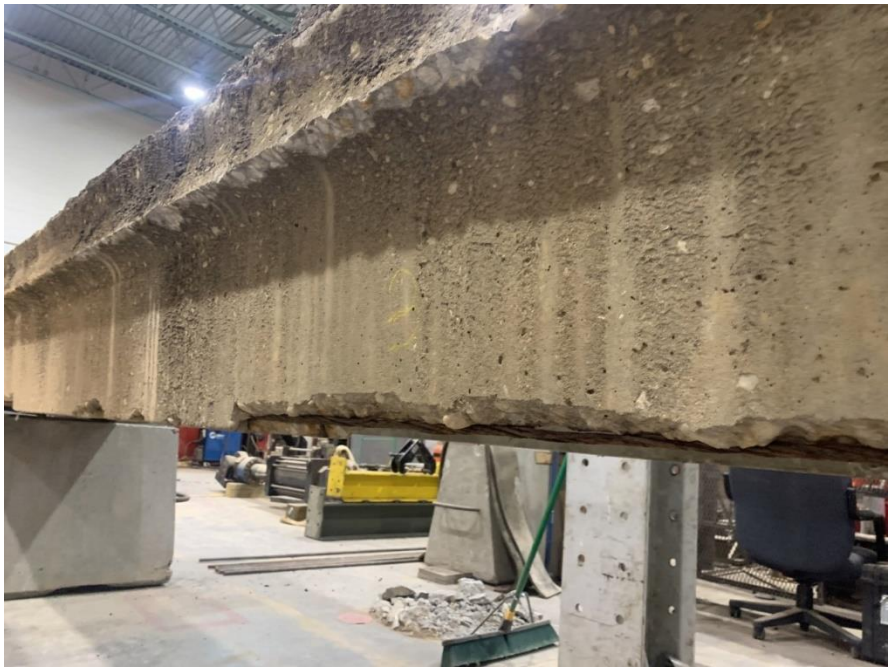

Figure A.24 C8 (NBI 3) strand corrosion near midspan.

Figure A.25 C8 (NBI 3) wide crack.

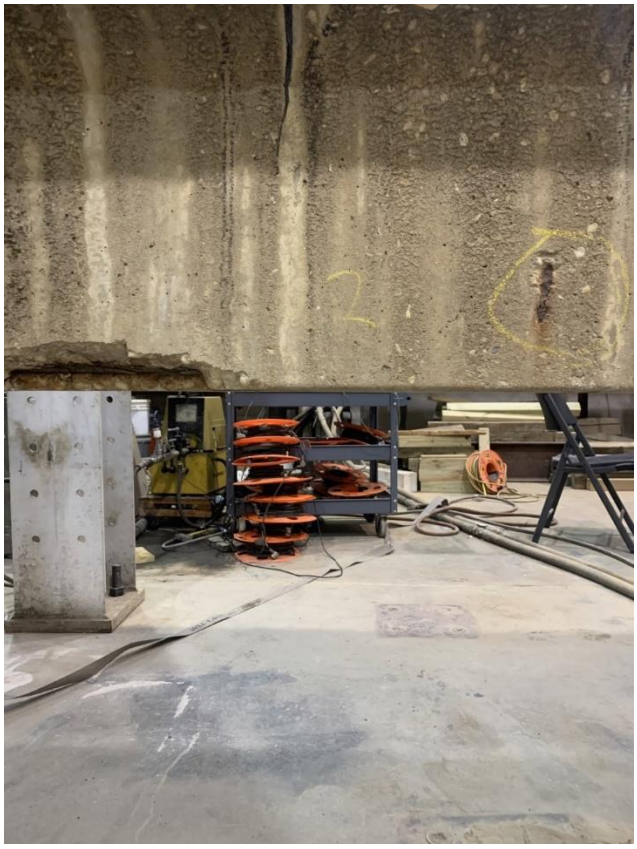

Figure A.26 C8 (NBI 3) moderate defect.

Figure A.27 C8 (NBI 3) minor defect.

Figure A.28 C9 (NBI 3) major defect.

Figure A.29 C9 (NBI 3) moderate defect near quarter span.

Figure A.30 C9 (NBI 3) moderate defect near midspan.

Figure A.31 C9 (NBI 3) major defect at midspan.

Figure A.32 C9 (NBI 3) major defect near midspan.

Figure A.33 C9 (NBI 3) medium crack, minor defect.

Figure A.34 C9 (NBI 3) large spall.

Figure A.35 C10 (NBI 2) medium crack.

Figure A.36 C10 (NBI 2) moderate defect near midspan.

Figure A.37 C10 (NBI 2) small spall.

Figure A.38 C10 (NBI 2) small spall.

Figure A.39 C10 (NBI 2) major defect, severely compromised.

Figure A.40 C10 (NBI 2) major defect.

Figure A.41 C10 (NBI 2) rust staining, moderate defect.

Figure A.42 C11 (NBI 6) small spalling.

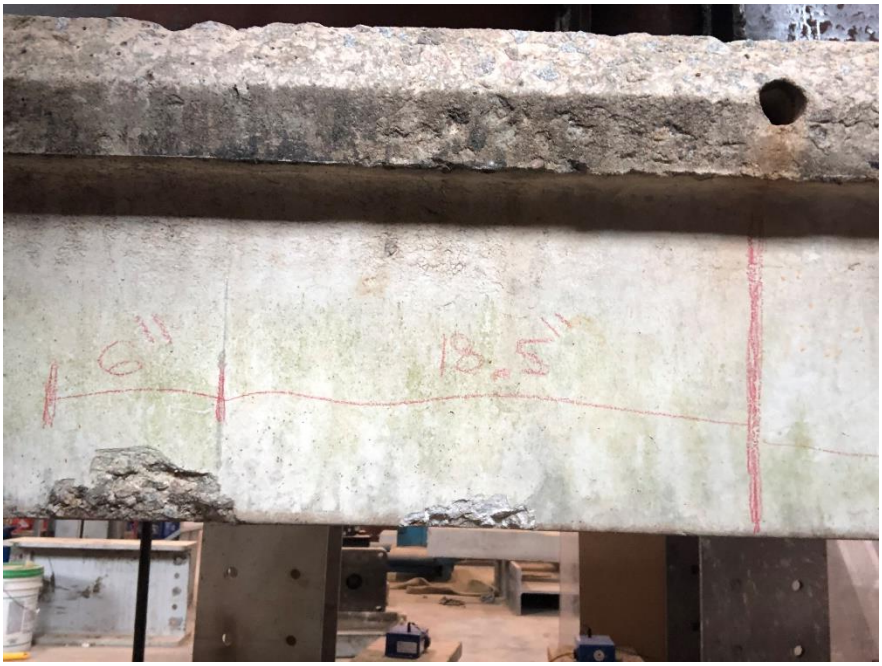

Figure A.43 C11 (NBI 6) small spalling near midspan.

Figure A.44 C11 (NBI 6) small spalling.

Figure A.45 C11 (NBI 6) large spalling.

Figure A.46 C11 (NBI 6) large spall near midspan.

Figure A.47 C11 (NBI 6) large spall near midspan.

Figure A.48 C12 (NBI 4) wide crack, moderate defect.

Figure A.49 C12 (NBI 4) wide crack near midspan.

Figure A.50 C12 (NBI 4) large and small spalling.

Figure A.51 C12 (NBI 4) end spalling.

Figure A.52 C13 (NBI 7) flange spalling.

Figure A.53 C13 (NBI 7)
flange spalling.

APPENDIX B: CALCULATIONS AND TABLES

Nominal Moment Calculation

Concrete:

Assume: f_c' = 5 ksi

f_{ci}' = 0.75 x 5 = 3.75 ksi

Strands:

A_S = 0.08 in.^{2}

No. of strands = 10

A_{ps} = 10 x 0.08 = 0.8 in.^{2}

Assume: f_{pu}= 250 ksi , E_p= 28500 ksi

f_{py} = 0.85 x 250 = 212.5 ksi (stress relieved strands)

Channel Properties:

B (flange width) = 33 in.

h_s *(flange thickness)* = 5 in.

b_{wb} *(bottom web width)* = 2.5 in.

b_{wu} *(upper web width)* = 4.5 in.

t_w *(web thickness)* = 12 in.

A_g= 249 in.^{2}

y_t = 5.2 in.

y_b = 11.8 in.

I_g= 4823 in.^{4}

S_t = 932 in.^{3}

S_b = 408 in.^{3}

d_p *(distance between top fiber and c.g. of strands)* = 17” – 4.375” = 12.7 in.

Analysis:

K_1 = 2(1.04 - $\frac{f_{py}}{f_{pu}}$) = 0.38

$\beta_1 = 0.85 - (0.05 * \frac{f'_c[psi]-4000}{1000})$ = 0.80 4000 < f'$_c$ [psi] < 8000

c = $\frac{A_{ps}f_{pu}}{0.85f'_c\beta_1 B - K_1 A_{ps}\frac{f_{pu}}{d_p}}$ = 1.69 in.

a = $\beta_1 * c$ = 1.35 in.

$f_{ps} = f_{pu}\left(1 - K_1 \frac{c}{d_p}\right)$ = 238 ksi

$M_n = A_{ps}f_{ps}\left(d_p - \frac{a}{2}\right)$ = 191 kip-ft. **compression steel neglected**

Material Properties

Table B.1 Strand tensile strength test results.

Specimen	Strand #	Ultimate Tensile Load (P_u) (lbs)	Ultimate Stress (σ_u) (ksi)****	P_u / P_{nu} ***	Strand Corrosion Condition Rating (1-4)**
C3	1	22450	281	1.12	1
	2	22450	281	1.12	1
C4	1	17180	NA	0.859	4
C8	1	14150	NA	0.708	3
	2	21910	274	1.10	2
C9	1	16760	NA	0.838	4
	2	23760	297	1.19	1
C10	1	18800	NA	0.940	4
	2	19460	NA	0.973	3
	3	23800	298	1.19	2
Other*	1	13720	NA	0.686	4
	2	23770	297	1.19	1
C11	1	23050	288	1.15	2
	2	23100	289	1.16	2

** 'Other' refers to a similar specimen not included in the testing described in this thesis*

***Corrosion condition: 1) no corrosion, 2) minimal to almost no corrosion, 3) corrosion with minor section loss, 4) corrosion and section loss*

**** P_{nu} = 250,000 psi * 0.08 in^2 = 20,000 lbs*

***** $\sigma_u = P_u / 0.08$ in^2. This was only considered for strands without section loss (condition 1 or 2)*

Table B.2 Statistics of strand tensile strength tests.

Statistic	
Average tensile stress of strands in condition 1:	289 ksi
Average tensile stress of strands in condition 2:	287 ksi
Average tensile stress of strands in condition 1 & 2:	288 ksi

Table B.3 Concrete compression test results.

Specimen	**Core #**	**D_1 (in.)**	**D_2 (in.)**	**Davg (in.)**	**Cross-Sectional Area (in.^{2})**	**Ultimate Load (P_u) (lbs)**	**f'_c (psi)**	**Failure Type**	**Average f'_c (psi)**
C9	1	2.045	2.041	2.043	3.28	34800	10620	1	10610
	2	2.044	2.042	2.043	3.28	40340	12310	1	
	3	2.040	2.048	2.044	3.28	29180	8893	4	
C10	1	2.038	2.037	2.038	3.26	37530	11510	5	10900
	2	2.043	2.041	2.042	3.27	35640	10880	2	
	3	2.040	2.042	2.041	3.27	33750	10320	4	
C8	1	2.040	2.046	2.043	3.28	38650	11790	1	10610
	2	2.040	2.042	2.041	3.27	37280	11390	2	
	3	2.038	2.043	2.041	3.27	28260	8642	3	
Other	1	2.087	2.083	2.085	3.41	20640	6045	5	8646
	2	2.083	2.087	2.085	3.41	42250	12370	2	
	3	2.085	2.085	2.085	3.41	17000	4979	5	
	4	2.090	2.090	2.090	3.43	38400	11190	2	
C11	1	2.097	2.087	2.092	3.44	38600	11230	2	9018
	2	2.094	2.062	2.078	3.39	33600	9907	4	
	3	2.085	2.007	2.046	3.29	15900	4836	1	
	4	2.095	2.094	2.095	3.45	34790	10100	2	
C12	1	2.091	2.090	2.091	3.43	32070	9343	3	9877
	2	2.090	2.083	2.087	3.42	33430	9777	2	
	3	2.094	2.075	2.085	3.41	35880	10510	2	

Notes:
'Other' refers to a similar specimen not included in the testing described in this thesis
D_1: Diameter one
D_2: Diameter two
D_{avg}: Average of diameter one and two
Failure Type: 1) well-formed cones on both ends, 2) well-formed cone with vertical cracks, 3) columnar vertical cracking, 4) diagonal fracture with no cracking, 5) side fracture at top or bottom corners, 6) similar to type 5 but end of cylinder is pointed. Refer to ASTM C 39/ C 39M for further clarification
$f'_c = P_u$ / cross-sectional area